A Kohn-Vogelius formulation to detect an obstacle immersed in a fluid

Fabien Caubet, Marc Dambrine, Djalil Kateb, Chahnaz Zakia Timimoun

A Kohn-Vogelius formulation to detect an obstacle immersed in a fluid

F Caubet[*], M Dambrine[†], D Kateb[‡] and C Z Timimoun [§]

February 12, 2012

Abstract

The aim of our work is to reconstruct an inclusion ω immersed in a fluid flowing in a larger bounded domain Ω via a boundary measurement on $\partial\Omega$. Here the fluid motion is assumed to be governed by the Stokes equations. We study the inverse problem of reconstructing ω thanks to the tools of shape optimization by minimizing a Kohn-Vogelius type cost functional. We first characterize the gradient of this cost functional in order to make a numerical resolution. Then, in order to study the stability of this problem, we give the expression of the shape Hessian. We show the compactness of the Riesz operator corresponding to this shape Hessian at a critical point which explains why the inverse problem is ill-posed. Therefore we need some regularization methods to solve numerically this problem. We illustrate those general results by some explicit calculus of the shape Hessian in some particular geometries. In particular, we solve explicitly the Stokes equations in a concentric annulus. Finally, we present some numerical simulations using a parametric method.

Keywords: geometric inverse problem, order two shape sensitivity, shape calculus, stationary Stokes problem.

AMS Subject Classification: 49Q10, 34A55, 49Q12

1   Introduction, notation and setting of the problem

The problem of reconstructing an inclusion ω immersed in a fluid flowing in a greater bounded domain Ω has been investigated by many authors. In [4], Alvarez *et al.* studied this inverse problem in order to determine the shape and the location of ω via the measurement of the velocity of the fluid and the Cauchy forces on the boundary $\partial\Omega$. After, in [5], Alves *et al.* used a method mainly based on the analysis of a system of nonlinear integral equations to determine the geometry and the position of a rigid object immersed in a viscous and incompressible fluid. In a more recent work [14], Conca *et al.* investigated the problem of the detection of a moving obstacle in a perfect fluid with a boundary measurement. When the obstacle is a ball, they showed that the position and the velocity

[*]Université de Pau et des pays de l'Adour, Laboratoire de Mathématiques Appliquées, Pau, France. `fabien.caubet@univ-pau.fr`

[†]Université de Pau et des pays de l'Adour, Laboratoire de Mathématiques Appliquées, Pau, France. `marc.dambrine@univ-pau.fr`

[‡]Université de Technologie de Compiègne, Laboratoire de Mathématiques Appliquées, Compiègne, France. `djalil.kateb@utc.fr`.

[§]Université d'Oran, Département de Mathématiques.   BP 1524, El-Menaouer, Oran, Algérie. `timimoun.chahnaz@univ-oran.dz`

of its center of mass can be identified from a single boundary measurement. In [15], using complex analysis tools, Conca *et al.* proved that this result cannot be generalized to any solid. However, they extended the result to moving ellipses: they proved that a solid with some symmetry properties can be partially detected. As expected for an inverse problem, the numerical experiments which were conducted show some difficulties to reconstruct the object. Those numerical difficulties are explained in a recent paper of Badra *et al.* (see [8]). Using a least-squares approach, the authors prove that the problem is severely ill-posed.

Here the fluid motion is assumed to be governed by the classical Stokes equations with non-homogeneous Dirichlet boundary condition on the exterior boundary and homogeneous Dirichlet boundary condition on the interior boundary. In order to simplify the expression, we assume that the exterior forces are null but the same results hold if we add a second member. This problem is classical and was studied by many authors (see for example [4], [8], [28], [1], [9, 10]) due to its importance in many applications involving fluid related technology and receive considerable attention by engineers and mathematicians. It is known to be ill-posed and our goal is to determine what sort of informations on the shape to be detected can be recovered by the tools of shape optimization.

Following previous works on electrical impedance tomography by Afraites *et al.* in [2] or [3] and Badra *et al.* in [8], we solve our inverse problem by minimizing a cost functional. In our paper, we consider an other approach than the least-squares cost functional for the same problem than the one studied in [8]. Indeed, we show how to solve the inverse problem by defining a Kohn-Vogelius type cost functional. Here we make the measurement only on a part of the exterior boundary and not on the whole exterior boundary as in the classical Kohn-Vogelius approach (see [2] for example). Thus, we consider here the Stokes equations with Dirichlet and mixed boundary conditions. Then, we follow the classical recipe: first we give an explicit formula for the gradient of this functional and compute after the associated shape Hessian to study the stability. We show the compactness of the Riesz operator corresponding to this shape Hessian at a critical point; this explains why the inverse problem is ill-posed. We then illustrate this result by computing explicitly this shape Hessian matrix for some particular geometries; we point out the consequence of the *high frequencies* on the value of the smallest eigenvalue. Finally, we present some numerical simulations with a regularization method: we use here a parametric model.

The paper is organized as follows. Firstly, we introduce the notations, the overdetermined problem that we consider and the Kohn-Vogelius cost functional J_{KV}. Secondly, in Section 2, we state the main results of this work. We recall an important identifiability result that we quote from Alvarez *et al.* (see [4, Theorem 1.2]) which ensures that the functional J_{KV} has a unique global minimum. The first order derivatives of the state and of the cost functional are characterized and the shape Hessian is explicitly computed. We then claim that the Riesz operator associated to the shape Hessian is compact. This result is crucial in the sense that it explains all the stability difficulties that one has to face. Finally, in order to illustrate the exponentially ill-posedness of this problem, we present an explicit calculus of the shape Hessian in a concentric annulus and compare it with the electrical impedance tomography case (*i.e.* the Laplacian case). In Section 3, we prove those results. In the last part of this paper, we present some numerical attempts to effectively reconstruct the inclusion ω using shape derivative informations. Let us point out that we use a parametric model of shape variation in order to highlight the bad conditioning of the Hessian matrix. To remove the oscillations due to the *high frequencies*, we propose an *adaptive method* which seems to be efficient. The needed results on Stokes equations with mixed boundary conditions (a theorem of existence and uniqueness of the solution and a local regularity result) are recalled in Appendix A. Moreover, the explicit computations

2

of the solution of the Stokes equations in an annulus are detailed in Appendix B.

Introduction of the general notations. Let us introduce the notations that we adopt in this paper. For a bounded Lipschitz open set $\Omega \subset \mathbb{R}^N$ ($N = 2$ or 3), we denote by $\mathrm{L}^p(\Omega)$, $\mathrm{W}^{m,p}(\Omega)$ and $\mathrm{H}^s(\Omega)$ the usual Lebesgue and Sobolev spaces. We note in bold the vectorial functions and spaces: $\mathbf{L}^p(\Omega)$, $\mathbf{W}^{m,p}(\Omega)$, $\mathbf{H}^s(\Omega)$, etc. We denote by $|\Omega|$ the measure of Ω. Moreover, $\mathbf{n}$ represents the external unit normal to $\partial\Omega$, and for a smooth enough function u, we note $\partial_{\mathbf{n}} u$ the normal derivative of u. Finally, we define the space

$$\mathrm{L}_0^2(\Omega) := \left\{ p \in \mathrm{L}^2(\Omega), \ \int_\Omega p = 0 \right\}.$$

The problem setting. Let Ω be a bounded, connected and Lipschitz open subset of $\mathbb{R}^N$ ($N = 2$ or 3). Let $d_0 > 0$ fixed (small). We define $\mathcal{O}_{d_0}$ the set of all open subsets ω of Ω with a $C^{2,1}$ boundary such that $\mathrm{d}(x, \partial\Omega) > d_0$ for all $x \in \omega$ and such that $\Omega\backslash\overline{\omega}$ is connected. The set $\mathcal{O}_{d_0}$ is referred as the set of admissible geometries. Notice that we make the assumption that the inclusion is far from the boundary $\partial\Omega$. We also define Ω_{d_0} an open set with a C^∞ boundary such that

$$\{x \in \Omega \,;\, \mathrm{d}(x, \partial\Omega) > d_0/2\} \subset \Omega_{d_0} \subset \{x \in \Omega \,;\, \mathrm{d}(x, \partial\Omega) > d_0/3\}.$$

Let $\boldsymbol{f} \in \mathbf{H}^{1/2}(\partial\Omega)$ such that $\boldsymbol{f} \neq \mathbf{0}$ satisfying the compatibility condition

$$\int_{\partial\Omega} \boldsymbol{f} \cdot \mathbf{n} = 0. \tag{1.1}$$

Let O be a non-empty subset of $\partial\Omega$ and $\boldsymbol{g} \in \mathbf{H}^{-1/2}(O)$ be an admissible boundary measurement. For $\omega \in \mathcal{O}_{d_0}$, let us consider the following overdetermined Stokes boundary value problem

$$\begin{cases} -\nu\Delta\boldsymbol{u} + \nabla p &=& \mathbf{0} & \text{in } \Omega\backslash\overline{\omega} \\ \operatorname{div}\boldsymbol{u} &=& 0 & \text{in } \Omega\backslash\overline{\omega} \\ \boldsymbol{u} &=& \boldsymbol{f} & \text{on } \partial\Omega \\ \boldsymbol{u} &=& \mathbf{0} & \text{on } \partial\omega \\ -\nu\partial_{\mathbf{n}}\boldsymbol{u} + p\mathbf{n} &=& \boldsymbol{g} & \text{on } O. \end{cases} \tag{1.2}$$

Here the constant $\nu > 0$ represents the *kinematic viscosity* of the fluid, the vectorial function $\boldsymbol{u}$ represents the velocity of the fluid and the scalar function p represents the pressure.

We assume here that there exists $\omega^* \in \mathcal{O}_{d_0}$ such that (1.2) has a solution. Thus, we consider the following geometric inverse problem:

find $\omega \in \mathcal{O}_{d_0}$ and a pair $(\boldsymbol{u}, p)$ which satisfy the overdetermined system (1.2). (1.3)

We will tackle the inverse problem of reconstructing ω thanks to the tools of shape optimization. In order to recover the shape of the inclusion ω, a usual strategy is then to minimize a cost functional. In this work, we consider the following Kohn-Vogelius cost functional

$$J_{KV}(\omega) := \frac{1}{2} \int_{\Omega\backslash\overline{\omega}} \nu \left| \nabla(\boldsymbol{u_D} - \boldsymbol{u_N}) \right|^2,$$

where $(\boldsymbol{u_D}, p_D) \in \mathbf{H}^1(\Omega\backslash\overline{\omega}) \times \mathrm{L}_0^2(\Omega\backslash\overline{\omega})$ is the unique solution of the Stokes problem with Dirichlet boundary conditions

$$\begin{cases} -\nu\Delta\boldsymbol{u_D} + \nabla p_D &= \boldsymbol{0} \quad \text{in } \Omega\backslash\overline{\omega} \\ \operatorname{div}\boldsymbol{u_D} &= 0 \quad \text{in } \Omega\backslash\overline{\omega} \\ \boldsymbol{u_D} &= \boldsymbol{f} \quad \text{on } \partial\Omega \\ \boldsymbol{u_D} &= \boldsymbol{0} \quad \text{on } \partial\omega \end{cases} \tag{1.4}$$

and $(\boldsymbol{u_N}, p_N) \in \mathbf{H}^1(\Omega\backslash\overline{\omega}) \times \mathrm{L}^2(\Omega\backslash\overline{\omega})$ is the unique solution of the Stokes problem with mixed boundary conditions

$$\begin{cases} -\nu\Delta\boldsymbol{u_N} + \nabla p_N &= \boldsymbol{0} \quad \text{in } \Omega\backslash\overline{\omega} \\ \operatorname{div}\boldsymbol{u_N} &= 0 \quad \text{in } \Omega\backslash\overline{\omega} \\ -\nu\partial_{\mathbf{n}}\boldsymbol{u_N} + p_N\mathbf{n} &= \boldsymbol{g} \quad \text{on } O \\ \boldsymbol{u_N} &= \boldsymbol{f} \quad \text{on } \partial\Omega\backslash\overline{O} \\ \boldsymbol{u_N} &= \boldsymbol{0} \quad \text{on } \partial\omega. \end{cases} \tag{1.5}$$

We refer to [12] or [18] for the results of existence, uniqueness and regularity of the solutions of the Stokes problem with Dirichlet boundary conditions. Notice that we assume the compatibility condition (1.1) associated to problem (1.4) is satisfied. Concerning the mixed boundary conditions, we recall the main results used in this paper in Appendix A. Hence, the existence and the uniqueness of the couple $(\boldsymbol{u_N}, p_N)$ is guaranteed by Theorem 11.

Then, we try to minimize the Kohn-Vogelius cost functional J_{KV}:

$$\omega^* = \underset{\omega\in\mathcal{O}_{d_0}}{\operatorname{argmin}} J_{KV}(\omega). \tag{1.6}$$

Indeed, if ω^* is solution of the inverse problem (1.3), then $J_{KV}(\omega^*) = 0$ and (1.6) holds. Conversely, if ω^* solves (1.6) with $J_{KV}(\omega^*) = 0$, then this domain ω^* is a solution of the inverse problem.

Introduction of the needed functional tools. To define the shape derivatives, we will use the velocity method introduced by Murat and Simon in 1976 in [23]. To this end, we need to introduce the space of admissible deformations

$$\boldsymbol{U} := \{\boldsymbol{\theta} \in \mathbf{W}^{3,\infty}(\mathbb{R}^N); \operatorname{Supp}\boldsymbol{\theta} \subset \overline{\Omega_{d_0}}\}.$$

Then for $\boldsymbol{V} \in \boldsymbol{U}$ and $t \in [0, T)$ (where $T > 0$ is a fixed real number sufficiently small), we define $\omega_t := (\mathbf{I} + t\,\boldsymbol{V})(\omega)$. In this paper, $\boldsymbol{V}$ is referred as the perturbation direction and we denote

$$V_{\mathrm{n}} := \boldsymbol{V} \cdot \mathbf{n}.$$

For details concerning the differentiation with respect to the domain, we refer to the papers of Simon [26, 27] and the books of Henrot and Pierre [20] and of Sokołowski and Zolsio [30].

2 Statement of main results

Identifiability result. We quote an identifiability result in the Dirichlet case proved by Alvarez *et al.* [4, Theorem 1.2]. In order to state it, let us precise a notation: we denote by σ the *stress tensor* defined by

$$\sigma(\boldsymbol{u}, p) := \nu(\nabla\boldsymbol{u} +^t \nabla\boldsymbol{u}) - p\mathrm{I}.$$

Here $^t\nabla\boldsymbol{u}$ is the transposed matrix of $\nabla\boldsymbol{u}$. Notice that if div $\boldsymbol{u} = 0$ in $\Omega\backslash\overline{\omega}$, one has

$$-\text{div}\,(\sigma(\boldsymbol{u}, p)) = -\nu\Delta\boldsymbol{u} + \nabla p \quad \text{in } \Omega\backslash\overline{\omega}.$$

Theorem 1 (Alvarez *et al.*, [4])**.** *Let $\Omega \subseteq \mathbb{R}^N$ ($N = 2$ or 3) be a bounded $C^{1,1}$ domain, and O a non-empty open subset of $\partial\Omega$. Let*

$$\omega_0, \omega_1 \in \{\omega \subset\subset \Omega;\ \omega \text{ is open, Lipschitz and } \Omega\backslash\overline{\omega} \text{ is connected}\}$$

and $\boldsymbol{f} \in \mathbf{H}^{3/2}(\partial\Omega)$ with $\boldsymbol{f} \neq \mathbf{0}$, satisfying the flux condition $\displaystyle\int_{\partial\Omega} \boldsymbol{f} \cdot \mathbf{n} = 0$. For $\varepsilon_* = 0$ or $\varepsilon_* = 1$, let $(\boldsymbol{u_j}, p_j)$ for $j = 0, 1$, be a solution of

$$\begin{cases} -\text{div}\,(\sigma(\boldsymbol{u_j}, p_j)) + \varepsilon_*\text{div}\,(\boldsymbol{u_j} \otimes \boldsymbol{u_j}) &=& \mathbf{0} & \text{in } \Omega\backslash\overline{\omega_j} \\ \text{div}\,\boldsymbol{u_j} &=& 0 & \text{in } \Omega\backslash\overline{\omega_j} \\ \boldsymbol{u_j} &=& \boldsymbol{f} & \text{on } \partial\Omega \\ \boldsymbol{u_j} &=& \mathbf{0} & \text{on } \partial\omega_j. \end{cases}$$

Assume that $(\boldsymbol{u_j}, p_j)$ are such that

$$\sigma(\boldsymbol{u_0}, p_0)\,\mathbf{n} = \sigma(\boldsymbol{u_1}, p_1)\,\mathbf{n} \quad \text{on } O.$$

Then $\omega_0 \equiv \omega_1$.

We can adapt this result to our problem, *i.e.* with $-\nu\partial_{\mathbf{n}}\boldsymbol{u} + p\mathbf{n}$ instead of $\sigma(\boldsymbol{u}, p)\mathbf{n}$, with $\varepsilon_* = 0$, with Ω Lipschitz and with $\boldsymbol{f} \in \mathbf{H}^{1/2}(\partial\Omega)$ (see [8, Theorem 2.2]). Hence this result states that given a fixed $\boldsymbol{f}$, two different geometries ω_0 and ω_1 in $\mathcal{O}_{d_0}$ yield two different measures $\boldsymbol{g_1}$ and $\boldsymbol{g_2}$. Thus problem (1.3) admits a unique solution.

Sensitivity with respect to the domain. The following result is based on [8, Propositions 2.1 and 2.5] and ensures that the solutions $(\boldsymbol{u_D}, p_D)$ and $(\boldsymbol{u_N}, p_N)$ are differentiable with respect to the domain. Moreover, we characterize the shape derivatives of these solutions.

Proposition 2 (First order shape derivatives of the states)**.** *Let $\boldsymbol{V} \in \boldsymbol{U}$ be an admissible deformation. The solutions $(\boldsymbol{u_D}, p_D)$ and $(\boldsymbol{u_N}, p_N)$ are differentiable with respect to the domain and the shape derivatives $(\boldsymbol{u'_D}, p'_D)$ and $(\boldsymbol{u'_N}, p'_N)$ belong to $\mathbf{H}^2(\Omega_{d_0}\backslash\overline{\omega}) \times \mathrm{H}^1(\Omega_{d_0}\backslash\overline{\omega})$. The couples $(\boldsymbol{u'_D}, p'_D) \in \mathbf{H}^1(\Omega\backslash\overline{\omega}) \times \mathrm{L}_0^2(\Omega\backslash\overline{\omega})$ and $(\boldsymbol{u'_N}, p'_N) \in \mathbf{H}^1(\Omega\backslash\overline{\omega}) \times \mathrm{L}^2(\Omega\backslash\overline{\omega})$ are respectively the only solutions of the following boundary value problems*

$$\begin{cases} -\nu\Delta\boldsymbol{u'_D} + \nabla p'_D &=& \mathbf{0} & \text{in } \Omega\backslash\overline{\omega} \\ \text{div}\,\boldsymbol{u'_D} &=& 0 & \text{in } \Omega\backslash\overline{\omega} \\ \boldsymbol{u'_D} &=& \mathbf{0} & \text{on } \partial\Omega \\ \boldsymbol{u'_D} &=& -V_{\mathrm{n}}\partial_{\mathbf{n}}\boldsymbol{u_D} & \text{on } \partial\omega \end{cases} \tag{2.1}$$

and

$$\begin{cases} -\nu\Delta\boldsymbol{u'_N} + \nabla p'_N &=& \mathbf{0} & \text{in } \Omega\backslash\overline{\omega} \\ \text{div}\,\boldsymbol{u'_N} &=& 0 & \text{in } \Omega\backslash\overline{\omega} \\ -\nu\partial_{\mathbf{n}}\boldsymbol{u'_N} + p'_N\mathbf{n} &=& \mathbf{0} & \text{on } O \\ \boldsymbol{u'_N} &=& \mathbf{0} & \text{on } \partial\Omega\backslash\overline{O} \\ \boldsymbol{u'_N} &=& -V_{\mathrm{n}}\partial_{\mathbf{n}}\boldsymbol{u_N} & \text{on } \partial\omega. \end{cases} \tag{2.2}$$

In order to simplify the expressions, we introduce the following notations:

$$\boldsymbol{w} := \boldsymbol{u_D} - \boldsymbol{u_N} \quad \text{and} \quad q := p_D - p_N, \tag{2.3}$$

where $(\boldsymbol{u_D}, p_D)$ solves (1.4) and $(\boldsymbol{u_N}, p_N)$ solves (1.5).

Proposition 3 (First order shape derivative of the functional). *For $\boldsymbol{V} \in \boldsymbol{U}$, the Kohn-Vogelius cost functional J_{KV} is differentiable at ω in the direction $\boldsymbol{V}$ with*

$$\mathrm{D}J_{KV}(\omega).\boldsymbol{V} = -\int_{\partial\omega} (\nu\partial_{\mathbf{n}}\boldsymbol{w} - q\mathbf{n}) \cdot \partial_{\mathbf{n}}\boldsymbol{u_D}V_{\mathrm{n}} + \frac{1}{2}\nu\int_{\partial\omega} |\nabla\boldsymbol{w}|^2 V_{\mathrm{n}}, \tag{2.4}$$

where $(\boldsymbol{w}, q)$ is defined by (2.3).

Second order analysis: justification of the instability. We study the stability of the problem. First, we give an explicit formula for the shape Hessian when $\omega \in \mathcal{O}_{d_0}$ in the following proposition. In order to simplify the expressions, we will use the following notations:

$$\boldsymbol{w}' := \boldsymbol{u_D'} - \boldsymbol{u_N'} \quad \text{and} \quad q' := p_D' - p_N', \tag{2.5}$$

where $(\boldsymbol{u_D'}, p_D')$ solves (2.1) and $(\boldsymbol{u_N'}, p_N')$ solves (2.2).

Proposition 4 (Second order shape derivative of the functional). *The solution $(\boldsymbol{u}, p)$ is twice differentiable with respect to the domain. Moreover, for $\boldsymbol{V} \in \boldsymbol{U}$, we have*

$$\mathrm{D}^2 J_{KV}(\omega).\mathbf{V}.\mathbf{V} = \int_{\partial\omega} \left[\nu\nabla\boldsymbol{w}' : \nabla\boldsymbol{w} - \left(\nu\partial_{\mathbf{n}}\boldsymbol{w}' + \nu\nabla\boldsymbol{w}\,\mathbf{n}' - q'\,\mathbf{n} - q\,\mathbf{n}'\right) \cdot \partial_{\mathbf{n}}\boldsymbol{u_D} \right.$$
$$\left. - \left(\nu\partial_{\mathbf{n}}\boldsymbol{w} - q\,\mathbf{n}\right) \cdot \left(\partial_{\mathbf{n}}\boldsymbol{u_D'} + \nabla\boldsymbol{u_D}\mathbf{n}'\right) \right] V_{\mathrm{n}}$$
$$+ \int_{\partial\omega} \mathrm{div}\left[\left(\frac{1}{2}\nu |\nabla\boldsymbol{w}|^2 - (\nu\partial_{\mathbf{n}}\boldsymbol{w} - q\,\mathbf{n}) \cdot \partial_{\mathbf{n}}\boldsymbol{u_D}\right)\boldsymbol{V} \right] V_{\mathrm{n}}, \tag{2.6}$$

where $(\boldsymbol{w}, q)$ and $(\boldsymbol{w}', q')$ are defined respectively by (2.3) and (2.5).

Let ω^* be a critical point of the Kohn-Vogelius functional. The following proposition shows that the optimization problem (1.6) is unstable.

Proposition 5 (Compactness at a critical point). *Let $\omega^* \in \mathcal{O}_{d_0}$ be a solution of the inverse problem (1.3). We have*

$$\mathrm{D}^2 J_{KV}(\omega^*).\mathbf{V}.\mathbf{V} = -\int_{\partial\omega^*} (\nu\partial_{\mathbf{n}}\boldsymbol{w}' - q'\,\mathbf{n}) \cdot \partial_{\mathbf{n}}\boldsymbol{u_D}V_{\mathrm{n}},$$

where $(\boldsymbol{w}', q')$ is defined by (2.5). Moreover, the Riesz operator corresponding to $\mathrm{D}^2 J_{KV}(\omega^*)$ defined from $\mathbf{H}^{1/2}(\partial\omega^*)$ to $\mathbf{H}^{-1/2}(\partial\omega^*)$ is compact.

The above proposition explains the difficulties encountered to solve numerically this problem. Indeed, the gradient has not a uniform sensitivity with respect to the deformation direction: hence, oscillations of the boundary generated by *high frequencies* are to be expected (see Section 4 for the numerical simulations).

Explicit computation of the shape Hessian when $O = \partial\Omega$. We illustrate the compact behavior of the shape Hessian in the case $O = \partial\Omega$. We study it in the bi-dimensional situation for some particular geometries. In order to simplify the expressions, we assume $\nu = 1$. In the following, $(\vec{e}_r, \vec{e}_\theta) := \left(\begin{pmatrix} \cos\theta \\ \sin\theta \end{pmatrix}, \begin{pmatrix} -\sin\theta \\ \cos\theta \end{pmatrix} \right)$ represents the polar coordinates system.

Proposition 6 (Explicit calculus of the shape Hessian in a concentric annulus). *Let us assume that the optimum ω^* corresponds to the concentric annulus case*

$$\Omega_\rho = \left\{ x \in \mathbb{R}^2, \, \rho < |x| < 1 \right\}.$$

Set $\boldsymbol{f} = \cos(n\theta)\vec{e}_r$, $n > 1$ and the associated Neumann boundary condition $\boldsymbol{g}$ (see (B.4)). Let $p > 1$ and let us define

$$
\begin{aligned}
\xi_n &:= \rho^2 - n^2\rho^{2n} + 2\left(-1 + n^2\right)\rho^{2+2n} - n^2\rho^{4+2n} + \rho^{2+4n} \\
\kappa_n &:= 2\left(-1 + \rho^{2n}\right) + n^2\left(-1 + \rho^2\right)\left(-1 + \rho^{2n}\right) - n\left(-1 + \rho^2\right)\left(1 + \rho^{2n}\right) \\
A_p &:= 2\left(-1 + \rho^{2p}\right)^2 + p^3\left(-1 + \rho^2\right)^2\left(-1 + \rho^{4p}\right) + 2p\left(1 + \rho^2\right)\left(-1 + \rho^{4p}\right) \\
&\quad - p^2\left(-1 + \rho^2\right)\left(1 + \rho^2 + 4\rho^{2p} + \rho^{4p} + \rho^{2+4p}\right) \\
B_p &:= \left(\rho^2 - p^2\rho^{2p} + 2\left(-1 + p^2\right)\rho^{2+2p} - p^2\rho^{4+2p} + \rho^{2+4p}\right) \\
&\quad \left(3\rho^2 + \left(8 + p^2\right)\rho^{2p} - 2\left(-1 + p^2\right)\rho^{2+2p} + p^2\rho^{4+2p} + 3\rho^{2+4p}\right).
\end{aligned}
$$

We have

$$\mathrm{D}^2 J_{KV}(\omega^*)\left[(\cos k\theta)\vec{e}_r, \, (\sin l\theta)\vec{e}_r\right] = 0$$

and

$$
\begin{aligned}
\mathrm{D}^2 J_{KV}(\omega^*)\left[(\cos k\theta)\vec{e}_r, \, (\cos l\theta)\vec{e}_r\right] &= \mathrm{D}^2 J_{KV}(\omega^*)\left[(\sin k\theta)\vec{e}_r, \, (\sin l\theta)\vec{e}_r\right] \\
&= \begin{cases} -\dfrac{1}{2}\left(R_{n,|n-k|} + R_{n,|n+l|}\right) & \text{if } k - l = 2n \\[2mm] -\dfrac{1}{2}\left(R_{n,|n+k|} + R_{n,|n-l|}\right) & \text{if } l - k = 2n \\[2mm] R_{n,|n+k|} + R_{n,|n-l|} & \text{if } k = l, \end{cases}
\end{aligned}
$$

where

$$
\begin{aligned}
R_{n,p} &:= \frac{-8\pi\rho^{2+2n}}{\xi_n^2}\kappa_n^2\frac{\rho^{2p}A_p}{B_p} \quad \text{if } p > 1 \\
R_{n,1} &:= -\frac{\pi\rho^{2n}}{\xi_n^2}\kappa_n^2\frac{-3 + 12\rho^2 - 6\rho^4 - 4\rho^6 + \rho^8 + 16\rho^4\ln(\rho)}{\left(-3 + 3\rho^2 - \rho^4 + \rho^6\right)\left(1 - \rho^2 + (1 + \rho^2)\ln(\rho)\right)} \\
R_{n,0} &:= 0.
\end{aligned}
$$

Remark 7. *In particular, if $|n - k| \notin \{0, 1\}$, notice that we can write the diagonal elements of the shape Hessian under the form*

$$
\begin{aligned}
\mathrm{D}^2 J_{KV}(\omega^*)\left[(\cos k\theta)\vec{e}_r, \, (\cos k\theta)\vec{e}_r\right] &= \mathrm{D}^2 J_{KV}(\omega^*)\left[(\sin k\theta)\vec{e}_r, \, (\sin k\theta)\vec{e}_r\right] \\
&= \frac{-8\pi\rho^{2+2n}}{\xi_n^2}\kappa_n^2\left(\frac{\rho^{2|n+k|}A_{|n+k|}}{B_{|n+k|}} + \frac{\rho^{2|n-k|}A_{|n-k|}}{B_{|n-k|}}\right)
\end{aligned}
$$

Let us compare our Stokes case with the electrical impedance tomography (E.I.T.) situation (see [2, Proposition 3]). We make the computations of the E.I.T. case with Dirichlet boundary conditions (in [2], they impose Neumann boundary conditions). Proceeding as

in [2] and in this paper, we prove that, in the E.I.T. situation with Dirichlet boundary conditions (and with $\boldsymbol{f} = \cos(n\theta)\vec{\boldsymbol{e}}_r$, $n > 1$), the Hessian matrix is defined similarly as in Proposition 6 with

$$
\begin{aligned}
R_{n,p} &:= \frac{-4\pi n^2 \rho^{-2+2n}}{(1-\rho^{2n})^2} \frac{p\rho^{2p}}{-1+\rho^{4p}} \quad \text{if } p \geq 1 \\
R_{n,0} &:= 0.
\end{aligned}
$$

Hence our shape Hessian has the same aspect than the Hessian in the E.I.T. case.

Example 8. *In order to be complete, we give some examples of the influence of the different parameters on the value of the smallest eigenvalue λ_1 of the shape Hessian $\mathrm{D}^2 J_{KV}(\omega^*)$ and hence on the reconstruction of the object.*

In Table 1, we study the influence of the size of the object ω^*. We here assume that $\boldsymbol{f} = \cos(2\theta)\vec{\boldsymbol{e}}_r$ (i.e. $n = 2$) and $k, l = 1, \ldots, 7$. The regularizing behavior is emphasized:

Table 1: Influence of the size of the object ρ on the smallest eigenvalue λ_1 of the shape Hessian $\mathrm{D}^2 J_{KV}(\omega^*)$.

ρ	0.9	0.7	0.5	0.3	0.1	0.05
λ_1	8.9401e+05	1.0921e+03	3.9992	0.0019	3.1851e-10	1.9032e-14

the more the object is far of the exterior boundary Ω, the more the functional is degenerated (and the more it is difficult to detect it).

In Table 2, we study the influence of the deformation directions. Here again we assume $n = 2$ and we fix $\rho = 0.7$. As we expected taking into account of our compactness result 5,

Table 2: Influence of the *high frequencies* on the smallest eigenvalue λ_1 of the shape Hessian $\mathrm{D}^2 J_{KV}(\omega^*)$.

k, l	1,...,5	1,...,10	1,...,15	1,...,30	1,...,40	1,...,60
λ_1	6.4483e+03	137.7707	14.5852	6.9862e-04	3.6934e-06	4.7546e-12

we see that the problem is severely ill-posed for the high frequencies.

In order to highlight this degeneracy and to compare our Stokes case with the E.I.T. case (with Dirichlet boundary conditions), we present in Figure 1 the spectrum of the shape Hessian matrix for 50 Fourier modes. Here again we fix $n = 2$ and $\rho = 0.7$. The results are presented in decimal logarithm scale to emphasize the behavior of the spectrum. As a clear consequence, the corresponding mode is poorly distinguished by the functional: the functional is almost flat in the direction of high frequencies. We will have to take into account of this point for the numerical simulations (see Section 4). Figure 1 also suggests that the E.I.T. case is as ill-posed as the Stokes case.

3 Proof of the main results

In order to simplify the expressions, we only detail the case $O = \partial\Omega$ but the proofs in the general case are simple adaptations of the ones detailed here. We recall that we use the notations $(\boldsymbol{w}, q)$ and $(\boldsymbol{w}', q')$ defined respectively by (2.3) and (2.5).
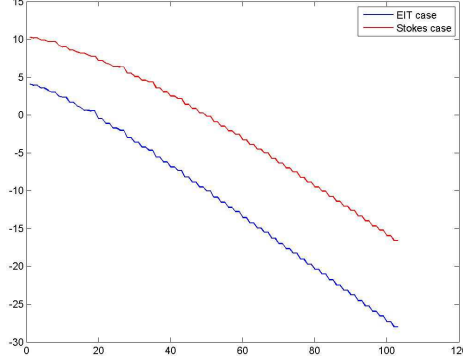
Figure 1: The typical spectrum of the shape Hessian in decimal logarithm scale

First order shape derivative. The proof of Proposition 2 is directly adapted of the proof of Proposition 2.5 in [8] and we refer to this paper for the details. The main difficulty is to prove the existence of the shape derivatives: it is obtained through a generalized implicit function theorem proved by Simon (see [28, Theorem 6]). The characterization of $(\boldsymbol{u'_D}, p'_D)$ and $(\boldsymbol{u'_N}, p'_N)$ is obtained using classical results of shape derivatives calculus (see [20, Chapter 5]).

Proof of Proposition 3. The Hadamard's formula (see [20, Theorem 5.2.2]) leads:

$$
\begin{aligned}
\mathrm{D}J_{KV}(\omega).\boldsymbol{V} &= \int_{\Omega\setminus\overline{\omega}} \left(\nu\nabla\boldsymbol{w} : \nabla\boldsymbol{w'} + \frac{1}{2}\nu\operatorname{div}\left(|\nabla\boldsymbol{w}|^2\,\boldsymbol{V}\right) \right) \\
&= \int_{\Omega\setminus\overline{\omega}} \nu\nabla\boldsymbol{w} : \nabla(\boldsymbol{u'_D} - \boldsymbol{u'_N}) + \frac{1}{2}\int_{\partial\omega} \nu\,|\nabla\boldsymbol{w}|^2\,V_{\mathrm{n}}
\end{aligned}
\tag{3.1}
$$

using the fact that $\boldsymbol{V} = \boldsymbol{0}$ on $\partial\Omega$. Let us prove that

$$
\int_{\Omega\setminus\overline{\omega}} \nu\nabla\boldsymbol{w} : \nabla\boldsymbol{u'_N} = 0.
\tag{3.2}
$$

Applying Green's Formula and using the system (2.2) solved by $(\boldsymbol{u'_N}, p'_N)$, we get

$$
\begin{aligned}
\int_{\Omega\setminus\overline{\omega}} \nu\nabla\boldsymbol{w} : \nabla\boldsymbol{u'_N} &= -\int_{\Omega\setminus\overline{\omega}} \nu\Delta\boldsymbol{u'_N}\cdot\boldsymbol{w} + \int_{\partial(\Omega\setminus\overline{\omega})} \nu\partial_{\mathbf{n}}\boldsymbol{u'_N}\cdot\boldsymbol{w} \\
&= -\int_{\Omega\setminus\overline{\omega}} \nabla p'_N\cdot\boldsymbol{w} + \int_{\partial(\Omega\setminus\overline{\omega})} \nu\partial_{\mathbf{n}}\boldsymbol{u'_N}\cdot\boldsymbol{w} \\
&= \int_{\Omega\setminus\overline{\omega}} p'_N\operatorname{div}\boldsymbol{w} - \int_{\partial(\Omega\setminus\overline{\omega})} p'_N\boldsymbol{w}\cdot\mathbf{n} + \int_{\partial(\Omega\setminus\overline{\omega})} \nu\partial_{\mathbf{n}}\boldsymbol{u'_N}\cdot\boldsymbol{w} \\
&= 0,
\end{aligned}
$$

since $\operatorname{div}\boldsymbol{w} = 0$ in $\Omega\setminus\overline{\omega}$, $-\nu\partial_{\mathbf{n}}\boldsymbol{u'_N} + p'_N\mathbf{n} = \boldsymbol{0}$ on $\partial\Omega$ and $\boldsymbol{w} = \boldsymbol{0}$ on $\partial\omega$.

Then, let us write $\displaystyle\int_{\Omega\setminus\overline{\omega}} \nu\nabla\boldsymbol{w} : \nabla\boldsymbol{u'_D}$ as an integral on $\partial\omega$. Proceeding as above, we

apply Green's Formula on this term and use the system (2.1) solved by $(\boldsymbol{u}'_{\boldsymbol{D}}, p'_D)$ to obtain

$$
\begin{aligned}
\int_{\Omega\backslash\overline{\omega}} \nu\nabla\boldsymbol{w} : \nabla\boldsymbol{u}'_{\boldsymbol{D}} &= -\int_{\Omega\backslash\overline{\omega}} \nu\Delta\boldsymbol{w}\cdot\boldsymbol{u}'_{\boldsymbol{D}} + \int_{\partial(\Omega\backslash\overline{\omega})} \nu\partial_{\mathbf{n}}\boldsymbol{w}\cdot\boldsymbol{u}'_{\boldsymbol{D}} \\
&= -\int_{\Omega\backslash\overline{\omega}} \nabla q\cdot\boldsymbol{u}'_{\boldsymbol{D}} + \int_{\partial(\Omega\backslash\overline{\omega})} \nu\partial_{\mathbf{n}}\boldsymbol{w}\cdot\boldsymbol{u}'_{\boldsymbol{D}} \\
&= \int_{\Omega\backslash\overline{\omega}} q\operatorname{div}\boldsymbol{u}'_{\boldsymbol{D}} - \int_{\partial(\Omega\backslash\overline{\omega})} q\,\boldsymbol{u}'_{\boldsymbol{D}}\cdot\mathbf{n} + \int_{\partial(\Omega\backslash\overline{\omega})} \nu\partial_{\mathbf{n}}\boldsymbol{w}\cdot\boldsymbol{u}'_{\boldsymbol{D}} \\
&= \int_{\partial(\Omega\backslash\overline{\omega})} (\nu\partial_{\mathbf{n}}\boldsymbol{w} - q\mathbf{n})\cdot\boldsymbol{u}'_{\boldsymbol{D}}.
\end{aligned}
$$

Since $\boldsymbol{u}'_{\boldsymbol{D}} = \mathbf{0}$ on $\partial\Omega$ and $\boldsymbol{u}'_{\boldsymbol{D}} = -\partial_{\mathbf{n}}\boldsymbol{u}_{\boldsymbol{D}}V_{\mathrm{n}}$ on $\partial\omega$, we obtain

$$
\int_{\Omega\backslash\overline{\omega}} \nu\nabla\boldsymbol{w} : \nabla\boldsymbol{u}'_{\boldsymbol{D}} = -\int_{\partial\omega} (\nu\partial_{\mathbf{n}}\boldsymbol{w} - q\mathbf{n})\cdot\partial_{\mathbf{n}}\boldsymbol{u}_{\boldsymbol{D}}V_{\mathrm{n}}. \tag{3.3}
$$

Gathering equations (3.1), (3.2) and (3.3), we check that

$$
\mathrm{D}J_{KV}(\omega).\boldsymbol{V} = -\int_{\partial\omega} (\nu\partial_{\mathbf{n}}\boldsymbol{w} - q\mathbf{n})\cdot\partial_{\mathbf{n}}\boldsymbol{u}_{\boldsymbol{D}}V_{\mathrm{n}} + \frac{1}{2}\nu\int_{\partial\omega} |\nabla\boldsymbol{w}|^2\,V_{\mathrm{n}}.
$$

$\square$

Characterization of the shape Hessian.

Proof of Proposition 4. The proof of the existence of the second order shape differentiability of the states $(\boldsymbol{u}_{\boldsymbol{D}}, p_D)$ and $(\boldsymbol{u}_{\boldsymbol{N}}, p_N)$ is directly adapted from [8, Proposition 2.3]. Thus we do not detail it here.

From Proposition 3, we have

$$
\begin{aligned}
\mathrm{D}J_{KV}(\omega).\boldsymbol{V} &= \int_{\partial\omega} \left[\frac{1}{2}\nu\,|\nabla\boldsymbol{w}|^2 - (\nu\partial_{\mathbf{n}}\boldsymbol{w} - q\mathbf{n})\cdot\partial_{\mathbf{n}}\boldsymbol{u}_{\boldsymbol{D}}\right]V_{\mathrm{n}} \\
&= \int_{\Omega\backslash\overline{\omega}} \operatorname{div}\left[\left(\frac{1}{2}\nu\,|\nabla\boldsymbol{w}|^2 - (\nu\partial_{\mathbf{n}}\boldsymbol{w} - q\mathbf{n})\cdot\partial_{\mathbf{n}}\boldsymbol{u}_{\boldsymbol{D}}\right)\boldsymbol{V}\right],
\end{aligned}
$$

since $\boldsymbol{V} \equiv \mathbf{0}$ on $\partial\Omega$. From Hadamard's formula (see [20, Theorem 5.2.2]), this leads

$$
\begin{aligned}
\mathrm{D}^2J_{KV}(\omega).\boldsymbol{V}.\boldsymbol{V} = \int_{\Omega\backslash\overline{\omega}} \operatorname{div}&\left(\left[\nu\nabla\boldsymbol{w}' : \nabla\boldsymbol{w} - (\nu\partial_{\mathbf{n}}\boldsymbol{w}' + \nu\nabla\boldsymbol{w}\mathbf{n}' - q'\mathbf{n} - q\mathbf{n}')\cdot\partial_{\mathbf{n}}\boldsymbol{u}_{\boldsymbol{D}} \right.\right. \\
&\left.\left. -(\nu\partial_{\mathbf{n}}\boldsymbol{w} - q\mathbf{n})\cdot(\partial_{\mathbf{n}}\boldsymbol{u}'_{\boldsymbol{D}} + \nabla\boldsymbol{u}_{\boldsymbol{D}}\mathbf{n}')\right]\boldsymbol{V}\right) \\
&+ \int_{\partial\omega} \operatorname{div}\left(\left[\frac{1}{2}\nu\,|\nabla\boldsymbol{w}|^2 - (\nu\partial_{\mathbf{n}}\boldsymbol{w} - q\mathbf{n})\cdot\partial_{\mathbf{n}}\boldsymbol{u}_{\boldsymbol{D}}\right]\boldsymbol{V}\right)V_{\mathrm{n}}.
\end{aligned}
$$

Since $\boldsymbol{V} = \mathbf{0}$ on $\partial\Omega$, we then obtain

$$
\begin{aligned}
\mathrm{D}^2J_{KV}(\omega).\boldsymbol{V}.\boldsymbol{V} = \int_{\partial\omega} &\left[\nu\nabla\boldsymbol{w}' : \nabla\boldsymbol{w} - (\nu\partial_{\mathbf{n}}\boldsymbol{w}' + \nu\nabla\boldsymbol{w}\mathbf{n}' - q'\mathbf{n} - q\mathbf{n}')\cdot\partial_{\mathbf{n}}\boldsymbol{u}_{\boldsymbol{D}}\right. \\
&\left. -(\nu\partial_{\mathbf{n}}\boldsymbol{w} - q\mathbf{n})\cdot(\partial_{\mathbf{n}}\boldsymbol{u}'_{\boldsymbol{D}} + \nabla\boldsymbol{u}_{\boldsymbol{D}}\mathbf{n}')\right]V_{\mathrm{n}} \\
&+ \int_{\partial\omega} \operatorname{div}\left(\left[\frac{1}{2}\nu\,|\nabla\boldsymbol{w}|^2 - (\nu\partial_{\mathbf{n}}\boldsymbol{w} - q\mathbf{n})\cdot\partial_{\mathbf{n}}\boldsymbol{u}_{\boldsymbol{D}}\right]\boldsymbol{V}\right)V_{\mathrm{n}}.
\end{aligned}
$$

$\square$

Justifying the ill-posedness of the problem. The instability of the inverse problem (1.3) is proved using the same methods as those used in [8]. Therefore, we use a local regularity argument (see Theorem 12) in order to prove the compactness of the Riesz operator corresponding to the shape Hessian at a solution of the inverse problem. An alternative proof could be to use the hydrodynamical potential layers as what is done in [2] for the Laplacian case.

In order to prove Proposition 5, we investigate the properties of stability of the cost functional J_{KV}. Then we consider an admissible inclusion $\omega^* \in \mathcal{O}_{d_0}$ which is solution of problem (1.3). Then, ω^* realizes the absolute minimum of the criterion J_{KV}, $J_{KV}(\omega^*) = 0$ and then $\boldsymbol{u_D} = \boldsymbol{u_N}$ and $p_D = p_N$ in $\Omega\backslash\overline{\omega}$. Therefore

$$\mathrm{D}^2 J_{KV}(\omega^*).\mathbf{V}.\mathbf{V} = -\int_{\partial\omega^*} (\nu\partial_\mathbf{n}\boldsymbol{w}' - q'\,\mathbf{n}) \cdot \partial_\mathbf{n}\boldsymbol{u_D}V_\mathrm{n}.$$

Proof of Proposition 5. We first decompose $\mathrm{D}^2 J_{KV}(\omega^*)$ as a composition of two operators: for $\boldsymbol{V} \in \boldsymbol{U}$,

$$\mathrm{D}^2 J_{KV}(\omega^*).\mathbf{V}.\mathbf{V} = \langle M(\boldsymbol{V}), T(\boldsymbol{V})\rangle_{\mathbf{H}^{-1/2}(\partial\omega^*),\mathbf{H}^{1/2}(\partial\omega^*)}$$

where $\langle\cdot,\cdot\rangle$ denote the dual product between $\mathbf{H}^{-1/2}(\partial\omega^*)$ and $\mathbf{H}^{1/2}(\partial\omega^*)$. Here, the operator $T : \mathbf{H}^{1/2}(\partial\omega^*) \to \mathbf{H}^{1/2}(\partial\omega^*)$ is defined by

$$T(\boldsymbol{V}) := -\partial_\mathbf{n}\boldsymbol{u_D}V_\mathrm{n}$$

and the operator $M : \mathbf{H}^{1/2}(\partial\omega^*) \to \mathbf{H}^{-1/2}(\partial\omega^*)$ is defined by

$$M(\boldsymbol{V}) := \nu\partial_\mathbf{n}\boldsymbol{w}' - q'\mathbf{n}.$$

From the systems (2.1) and (2.2) and using the fact that $\boldsymbol{u_D} = \boldsymbol{u_N}$ in $\Omega\backslash\overline{\omega^*}$ (and then $\partial_\mathbf{n}\boldsymbol{u_D} = \partial_\mathbf{n}\boldsymbol{u_N}$ on $\partial\omega^*$), we obtain the following system:

$$\begin{cases} -\nu\Delta\boldsymbol{w}' + \nabla q' &= \mathbf{0} &\text{in } \Omega\backslash\overline{\omega^*} \\ \mathrm{div}\,\boldsymbol{w}' &= 0 &\text{in } \Omega\backslash\overline{\omega^*} \\ \boldsymbol{w}' &= -\boldsymbol{u}'_N &\text{on } \partial\Omega \\ \boldsymbol{w}' &= \mathbf{0} &\text{on } \partial\omega^*. \end{cases}$$

Since $\partial_\mathbf{n}\boldsymbol{u_D}$ does not depend on $\boldsymbol{V}$, notice that the operator T is linear continuous as multiplier by a smooth function (see [22]). Now, let us prove the following lemma which states that the operator M is compact. Hence, the Riesz operator corresponding to the shape Hessian is compact as composition of linear continuous operator with a compact one. $\square$

Lemma 9. *The operator M is compact.*

Proof. We decompose the operator M as follows:

$$M := M_2 \circ M_1$$

with

$$M_1 : \boldsymbol{V} \in \mathbf{H}^{1/2}(\partial\omega^*) \mapsto M_1(\boldsymbol{V}) := -\boldsymbol{u}'_N \in \mathbf{H}^{1/2}(\partial\Omega),$$

and

$$M_2 : \boldsymbol{\Psi} \in \mathbf{H}^{1/2}(\partial\Omega) \mapsto M_2(\boldsymbol{\Psi}) := \nu\partial_\mathbf{n}\boldsymbol{\Phi} - \chi\mathbf{n} \in \mathbf{H}^{-1/2}(\partial\omega^*),$$

where $(\boldsymbol{u}'_N, p'_N)$ is solution of (2.2) and where $(\boldsymbol{\Phi}, \chi) \in \mathbf{H}^1(\Omega \backslash \overline{\omega^*}) \times \mathrm{L}_0^2(\Omega \backslash \overline{\omega^*})$ solves

$$
\begin{cases}
-\nu \Delta \boldsymbol{\Phi} + \nabla \chi & = \ \mathbf{0} \quad \text{in } \Omega \backslash \overline{\omega^*} \\
\operatorname{div} \boldsymbol{\Phi} & = \ 0 \quad \text{in } \Omega \backslash \overline{\omega^*} \\
\boldsymbol{\Phi} & = \ \boldsymbol{\Psi} \quad \text{on } \partial \Omega \\
\boldsymbol{\Phi} & = \ \mathbf{0} \quad \text{on } \partial \omega^*.
\end{cases} \tag{3.4}
$$

Let us prove that M_1 is linear continuous and M_2 is compact. We check that

$$M_1 = M_{1,2} \circ M_{1,1}$$

with

$$M_{1,1} : \boldsymbol{V} \in \mathbf{H}^{1/2}(\partial \omega^*) \mapsto M_{1,1}(\boldsymbol{V}) := -\partial_{\mathbf{n}} \boldsymbol{u_N} V_{\mathrm{n}} \in \mathbf{H}^{1/2}(\partial \omega^*)$$

and with

$$M_{1,2} : \boldsymbol{\eta} \in \mathbf{H}^{1/2}(\partial \omega^*) \mapsto M_{1,2}(\boldsymbol{V}) := -\boldsymbol{z} \in \mathbf{H}^{1/2}(\partial \Omega),$$

where the couple $(\boldsymbol{z}, q) \in \mathbf{H}^1(\Omega \backslash \overline{\omega^*}) \times \mathrm{L}^2(\Omega \backslash \overline{\omega^*})$ is solution of

$$
\begin{cases}
-\nu \Delta \boldsymbol{z} + \nabla q & = \ \mathbf{0} \quad \text{in } \Omega \backslash \overline{\omega^*} \\
\operatorname{div} \boldsymbol{z} & = \ 0 \quad \text{in } \Omega \backslash \overline{\omega^*} \\
-\nu \partial_{\mathbf{n}} \boldsymbol{z} + q \mathbf{n} & = \ \mathbf{0} \quad \text{on } \partial \Omega \\
\boldsymbol{z} & = \ \boldsymbol{\eta} \quad \text{on } \partial \omega^*.
\end{cases}
$$

Since $\partial_{\mathbf{n}} \boldsymbol{u_N}$ does not depend on $\boldsymbol{V}$, the operator $M_{1,1}$ is linear continuous as multiplier by a smooth function (see [22]) and the operator $M_{1,2}$ is clearly linear continuous. Thus M_1 is linear continuous.

Finally, we decompose M_2 as follows:

$$M_2 = M_{2,3} \circ M_{2,2} \circ M_{2,1}$$

where

$$M_{2,1} : \boldsymbol{\Psi} \in \mathbf{H}^{1/2}(\partial \Omega) \mapsto (\boldsymbol{\Phi}, \chi) \in \mathbf{H}^3(\Omega_{d_0} \backslash \overline{\omega^*}) \times \mathrm{H}^2(\Omega_{d_0} \backslash \overline{\omega^*})$$

with $(\boldsymbol{\Phi}, \chi)$ solution of (3.4),

$$M_{2,2} : (\boldsymbol{v}, \xi) \in \mathbf{H}^3(\Omega_{d_0} \backslash \overline{\omega^*}) \times \mathrm{H}^2(\Omega_{d_0} \backslash \overline{\omega^*}) \mapsto \nu \partial_{\mathbf{n}} \boldsymbol{v} - \xi \mathbf{n} \in \mathbf{H}^{3/2}(\partial \omega^*)$$

and $M_{2,3}$ is the compact imbedding of $\mathbf{H}^{3/2}(\partial \omega^*)$ into $\mathbf{H}^{-1/2}(\partial \omega^*)$. From the local regularity theorem 12, the operator $M_{2,1}$ is linear continuous and the operator $M_{2,2}$ is clearly linear continuous. Then, by composition M_2 is compact, which concludes the proof. $\square$

Explicit computation of the Hessian matrix in a concentric annulus. We recall that $(\vec{\boldsymbol{e}}_r, \vec{\boldsymbol{e}}_\theta) := \left(\begin{pmatrix} \cos \theta \\ \sin \theta \end{pmatrix}, \begin{pmatrix} -\sin \theta \\ \cos \theta \end{pmatrix} \right)$ represents the polar coordinates system.

Proof of Proposition 6. Using the computations of $\boldsymbol{u_D}, \boldsymbol{u_N}, \boldsymbol{u'_D}$ and $\boldsymbol{u'_N}$ (see Appendix B), we will compute the elements of the Hessian $\mathrm{D}^2 J_{KV}((\cos k\theta)\vec{\boldsymbol{e}_r}, (\cos l\theta)\vec{\boldsymbol{e}_r})$ when the Dirichlet data on the exterior boundary is taken as $\boldsymbol{f} = \boldsymbol{f}^{(ext)} = \cos(n\theta)\vec{\boldsymbol{e}_r}$. From the computations detailed in Appendix B, we see that only the elements with $k = l$ or $| k - l | = 2n$ have to be computed; the other elements are zero.

Let us begin by the case $k = l$. We have

$$
\begin{aligned}
\mathrm{D}^2 J_{KV}((\cos k\theta)\vec{\boldsymbol{e}_r}, (\cos k\theta)\vec{\boldsymbol{e}_r}) & = \ \langle -\partial_{\mathbf{n}}(\boldsymbol{u'_N} - \boldsymbol{u'_D}) + (p'_N - p'_D)\mathbf{n}(\rho, \theta), -V_{\mathrm{n}} \partial_{\mathbf{n}} \boldsymbol{u_D} \rangle \\
& = \ \int_{\partial \omega^*} (E + F),
\end{aligned}
$$

12

with

$$E(\theta) = \left(\widetilde{K}_{|n+k|,r} \cos{(n+k)\theta} + \widetilde{K}_{|n-k|,r} \cos{(n-k)\theta} \right) \left(K_{n,r}^{D} \cos{(n+k)\theta} + K_{n,r}^{D} \cos{(n-k)\theta} \right)$$

and with

$$F(\theta) = \left(\widetilde{L}_{|n+k|,r} \sin{(n+k)\theta} + \widetilde{L}_{|n-k|,r} \sin{(n-k)\theta} \right) \left(L_{n,r}^{D} \sin{(n+k)\theta} + L_{n,r}^{D} \sin{(n-k)\theta} \right),$$

where $K_{n,r}^{D}$ and $L_{n,r}^{D}$ are defined by (B.5) and $\widetilde{K}_{n,r}$ and $\widetilde{L}_{n,r}$ by (B.6). Since $K_{n,r}^{D} = 0$ by computations, we have $E(\theta) = 0$ and then we have only to compute

$$
\begin{aligned}
\mathrm{D}^2 J_{KV}((\cos k\theta)\vec{e_r}\,,\,(\cos k\theta)\vec{e_r}) &= \rho \int_0^{2\pi} (E(\theta) + F(\theta))d\theta \\
&= \pi\rho\left(\widetilde{L}_{|n+k|,r} L_{n,r}^{D} + \widetilde{L}_{|n-k|,r} L_{n,r}^{D} \right)
\end{aligned}
$$

Set $p_1 = |n+k|$ and $p_2 = |n-k|$. Defining ξ_n, κ_n, A_{p_i}, B_{p_i} and R_{n,p_i} as in the statement of Proposition 6, we obtain after some computations

$$\mathrm{D}^2 J_{KV}((\cos k\theta)\vec{e_r}\,,\,(\cos k\theta)\vec{e_r}) = R_{n,p_1}(\rho) + R_{n,p_2}(\rho).$$

Similarly, we prove that

$$\mathrm{D}^2 J_{KV}((\sin k\theta)\vec{e_r}\,,\,(\sin k\theta)\vec{e_r}) = R_{n,p_1}(\rho) + R_{n,p_2}(\rho).$$

Let us now study the case $|k - l| = 2n$. Set $\boldsymbol{V} := (\cos k\theta)\,\vec{e_r}$ and $\boldsymbol{W} := (\cos l\theta)\,\vec{e_r}$. We denote $(\boldsymbol{w}'_{\boldsymbol{W}}, q'_{\boldsymbol{W}})$ the shape derivative in the direction $\boldsymbol{W}$ (the pair $(\boldsymbol{w}', q')$ is defined in (2.5)). Then, using the linearity of the Stokes problem and the polarization formula for the quadratic form, we prove that

$$
\begin{aligned}
\mathrm{D}^2 J_{KV}((\cos k\theta)\vec{e_r}\,,\,(\cos l\theta)\vec{e_r}) = \\
\frac{1}{2}\left(\int_{\partial\omega^*} (-\partial\boldsymbol{w}'_{\boldsymbol{W}} + q'_{\boldsymbol{W}}\mathbf{n}) \cdot \partial_\mathbf{n}\boldsymbol{u}_D V_n + \int_{\partial\omega^*} (-\partial\boldsymbol{w}'_{\boldsymbol{V}} + q'_{\boldsymbol{V}}\mathbf{n}) \cdot \partial_\mathbf{n}\boldsymbol{u}_D W_n \right).
\end{aligned}
$$

Let us focus on the first integral: the case of the second integral is obtained by reversing the roles of k and l. Defining

$$G(\theta) = \left(\widetilde{K}_{|n+k|,r} \cos{(n+k)\theta} + \widetilde{K}_{|n-k|,r} \cos{(n-k)\theta} \right) \left(K_{n,r}^{D} \cos{(n+l)\theta} + K_{n,r}^{D} \cos{(n-l)\theta} \right)$$

and

$$H(\theta) = \left(\widetilde{L}_{|n+k|,r} \sin{(n+k)\theta} + \widetilde{L}_{|n-k|,r} \sin{(n-k)\theta} \right) \left(L_{n,r}^{D} \sin{(n+l)\theta} + L_{n,r}^{D} \sin{(n-l)\theta} \right),$$

we have

$$\int_{\partial\omega^*} (-\partial\boldsymbol{w}'_{\boldsymbol{W}} + q'_{\boldsymbol{W}}\mathbf{n}) \cdot \partial_\mathbf{n}\boldsymbol{u}_D V_n = \int_{\partial\omega^*} (G + H)\,.$$

Using the fact that $K_{n,r}^{D} = 0$, we then obtain

- if $k - l = 2n$

$$\int_{\partial\omega^*} (G + H) = \rho\widetilde{L}_{|n-k|,r} L_{n,r}^{D} \int_0^{2\pi} (\sin(n - k)\theta) \sin((n + l)\theta) = -\rho\pi\widetilde{L}_{|n-k|,r} L_{n,r}^{D},$$

13

- if $l - k = 2n$

$$\int_{\partial\omega^*} (G + H) = \rho\widetilde{L}_{|n+k|,r} L_{n,r}^D \int_0^{2\pi} (\sin(n+k)\theta)\sin((n-l)\theta) = -\rho\pi\widetilde{L}_{|n+k|,r} L_{n,r}^D.$$

Thus,

$$\mathrm{D}^2 J_{KV}(\omega^*) \left[(\cos k\theta)\vec{e_r}, (\cos l\theta)\vec{e_r}\right] = \begin{cases} -\dfrac{\rho\pi}{2} L_{n,r}^D \left(\widetilde{L}_{n,|n-k|} + \widetilde{L}_{n,|n+l|}\right) & \text{if } k - l = 2n \\[2mm] -\dfrac{\rho\pi}{2} L_{n,r}^D \left(\widetilde{L}_{n,|n+k|} + \widetilde{L}_{n,|n-l|}\right) & \text{if } l - k = 2n \\[2mm] \rho\pi L_{n,r}^D \left(\widetilde{L}_{n,|n+k|} + \widetilde{L}_{n,|n-l|}\right) & \text{if } k = l. \end{cases}$$

We proceed in the same way for $\mathrm{D}^2 J_{KV}(\omega^*) \left[(\sin k\theta)\vec{e_r}, (\sin l\theta)\vec{e_r}\right]$. $\qquad\square$

4 Numerical experiments

Since the problem is severely ill-posed, we need some regularization methods to solve it numerically, for example by adding to the functional a penalization in terms of the perimeter. Indeed, this term leads to well posed problems (see [13] or [16]). Here we choose to make a parametric regularization using a parametric model of shape variations in order to first highlight the bad conditioning of the shape Hessian matrix.

4.1 Framework for the numerical simulations

The numerical simulations presented are made in dimension two using the finite elements library MÉLINA (see [21]) and the mesh generator TRIANGLE (see [25]). We use a *P3-P2* finite elements discretization to solve the Stokes equations (1.4) and (1.5). The framework is the following: we assume the kinematic viscosity ν is equal to 1, the exterior boundary is assumed to be the unit circle centered at the origin and we consider the exterior Dirichlet boundary condition

$$\boldsymbol{f} := \begin{pmatrix} \mathrm{n}_2 \\ -\mathrm{n}_1 \end{pmatrix} = \left\{ \begin{pmatrix} \sin\theta \\ -\cos\theta \end{pmatrix}, \theta \in [0, 2\pi) \right\},$$

where $\mathbf{n} = (\mathrm{n}_1, \mathrm{n}_2)$ is the exterior unit normal. Notice that $\boldsymbol{f}$ is such that the compatibility condition (1.1) is satisfied. In order to have a suitable pair (*measure $\boldsymbol{g}$, domain ω^**), we use a synthetic data: we fix a shape ω^*, solve the Stokes problem (1.4) in $\Omega\backslash\overline{\omega^*}$ using another finite elements method (here a *P4-P3* finite elements discretization) and extract the measurement $\boldsymbol{g}$ by computing $-\nu\partial_{\mathbf{n}}\boldsymbol{u} + p\,\mathbf{n}$ on $\partial\Omega$. Except when mentioned, the simulations are performed in the case where $O = \partial\Omega$.

Here, we restrict ourselves to star-shaped domains and use polar coordinates for parametrization: the boundary $\partial\omega$ of the object can be then parametrized by

$$\partial\omega = \left\{ \begin{pmatrix} x_0 \\ y_0 \end{pmatrix} + r(\theta) \begin{pmatrix} \cos\theta \\ \sin\theta \end{pmatrix}, \ \theta \in [0, 2\pi) \right\},$$

where $x_0, y_0 \in \mathbb{R}$ and where r is a $C^{2,1}$ function, 2π-periodic and without double point. Taking into account of our main compactness result (Proposition 5), we approximate the polar radius r by its truncated Fourier series

$$r_N(\theta) := a_0^N + \sum_{k=1}^N a_k^N \cos(k\theta) + b_k^N \sin(k\theta),$$

14

for the numerical simulations. Indeed this regularization by projection permits to remove *high frequencies* generated by $\cos(k\theta)$ and $\sin(k\theta)$ for $k >> 1$, for which the functional is degenerated.

Then, the unknown shape is entirely defined by the coefficients (a_i, b_i). Hence, for $k = 1, \ldots, N$, the corresponding deformation directions are respectively,

$$\boldsymbol{V}_1 := \boldsymbol{V}_{x_0} := \begin{pmatrix} 1 \\ 0 \end{pmatrix}, \quad \boldsymbol{V}_2 := \boldsymbol{V}_{y_0} := \begin{pmatrix} 0 \\ 1 \end{pmatrix}, \quad \boldsymbol{V}_3(\theta) := \boldsymbol{V}_{a_0}(\theta) := \begin{pmatrix} \cos\theta \\ \sin\theta \end{pmatrix},$$

$$\boldsymbol{V}_{2k+2}(\theta) := \boldsymbol{V}_{a_k}(\theta) := \cos(k\theta) \begin{pmatrix} \cos\theta \\ \sin\theta \end{pmatrix}, \quad \boldsymbol{V}_{2k+3}(\theta) := \boldsymbol{V}_{b_k}(\theta) := \sin(k\theta) \begin{pmatrix} \cos\theta \\ \sin\theta \end{pmatrix},$$

$\theta \in [0, 2\pi)$. The gradient is then compute component by component using its characterization (see Proposition 3, formula (2.4)):

$$\left(\nabla J_{KV}(\omega)\right)_k = \mathrm{D}J_{KV}(\omega) \cdot \boldsymbol{V}_k, \qquad k = 1, \ldots, 2N + 3.$$

This equality is simply that

$$\lim_{t \to 0} \frac{J_{KV}\big((\mathbf{I} + t\boldsymbol{V}_k)(\omega)\big) - J_{KV}(\omega)}{t} = \mathrm{D}J_{KV}(\omega) \cdot \boldsymbol{V}_k.$$

Notice that we have to solve only two Stokes problems (problems (1.4) and (1.5)) to compute the gradient. Indeed, the directional perturbations $\boldsymbol{V}$ dependance is explicit in formula (2.4).

The optimization method used for the numerical simulations is here the classical gradient algorithm with a line search (using the Wolfe conditions: see for example [24, eq. (3.6) page 34]). Moreover, we here use $N_{ext} := 100$ discretization points for the exterior boundary and $N_{int} := 75$ for the interior boundary. In order to be completely explicit, we detail this algorithm:

Algorithm 1
1. fix a number of iterations M and an initial shape ω_0,
2. mesh $\Omega \backslash \overline{\omega_i}$ using TRIANGLE (where ω_i denotes the ith iterate of the approximate shape),
3. solve problems (1.4) and (1.5) with $\omega = \omega_i$ using MÉLINA,
4. extract $\nabla \boldsymbol{u_D}$, $\nabla \boldsymbol{u_N}$, p_D and p_N on $\partial \omega_i$ and compute $\nabla J_{KV}(\omega_i)$ using formula (2.4),
5. use the Wolfe conditions to compute a satisfying step length α_i,
6. move the coefficients associated to the shape: $\omega_{i+1} = \omega_i - \alpha_i \nabla J_{KV}(\omega_i)$,
7. get back to the step 2. while $i < M$.

Remark 10. *Here, we do not use an optimization method of order two due to the expression of the shape Hessian (2.6). Indeed, notice that $(\boldsymbol{u'_D}, p'_D)$ and $(\boldsymbol{u'_N}, p'_N)$ (and so $(\boldsymbol{w'}, q'))$ depend on the perturbation direction $\boldsymbol{V}$. Therefore, if we want to compute this shape Hessian (for a shape parametrized by k parameters), then we will have to solve $2 + 2 * k$ Stokes problems, which would be too costly.*

4.2 Highlight of the degeneration of the functional

First, we want to detect an obstacle ω_1^* contained in the class of objects with which we work. We want to detect the obstacle which boundary is parametrized by:

$$\partial \omega_1^* = \left\{ \begin{pmatrix} 0.15 \\ 0.15 \end{pmatrix} + \big(0.65 - 0.25 \cos\theta - 0.15 \sin\theta\big) \begin{pmatrix} \cos\theta \\ \sin\theta \end{pmatrix}, \theta \in [0, 2\pi) \right\},$$

that is to say with five parameters. In order to reconstruct this object, we work with shapes parametrized respectively by five and fifteen parameters and we stop each experiment when we obtain a residual value of the cost function J_{KV}: $\varepsilon \approx 10^{-3}$. Figure 2 shows that when
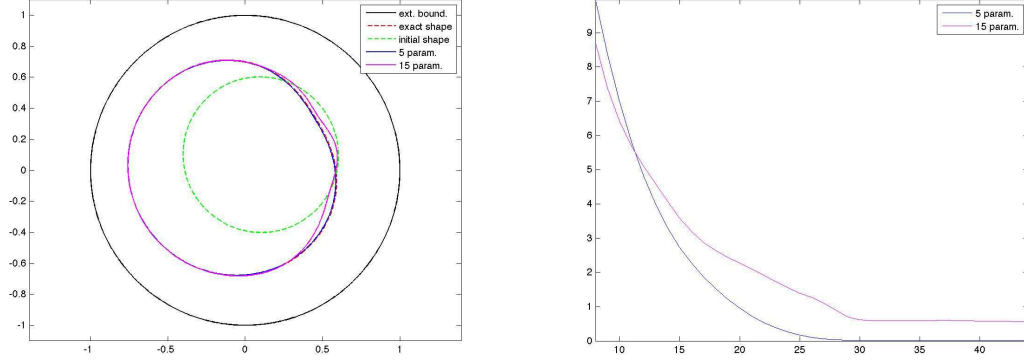

Figure 2: Reconstruction of ω_1^* with different numbers of parameters

we work with five parameters, the residual ε corresponds to a very good approximation of the object. But the more we add parameters, the more the functional flattens and the more the approximation corresponding to the residual ε is poor. Indeed, we see oscillations of the final object when we work with *high frequencies*. We can also notice that it is longer to obtain the residual ε with many parameters.

The same experiment was conducted to detect a more complicated obstacle which does not belong to the discretized set of objects. It is parametrized by:

$$\partial\omega_2^* = \left\{ \begin{pmatrix} 0.1 + 0.5\cos\theta + 0.1\cos 4\theta \\ 0.5\sin\theta + 0.1\cos 4\theta \end{pmatrix}, \, \theta \in [0, 2\pi) \right\}. \tag{4.1}$$

Here again, the conclusion is the same (see Figure 3): *high frequencies* lead oscillations of
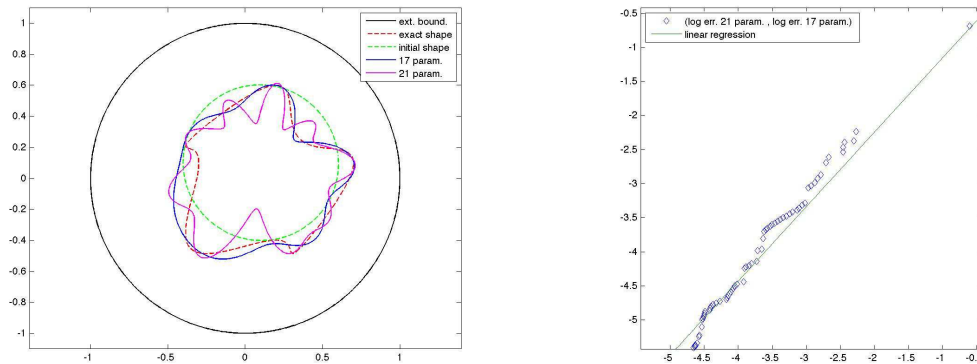

Figure 3: Reconstruction of ω_2^* with different numbers of parameters

the boundary and then a poorer approximation.

Here again, more iterations are needed to obtain the residual ε. In order to compare the errors, we represent on the second graph of Figure 3 the logarithm of the residual obtained with 17 parameters (noted $\log(J_{17})$) versus the logarithm of the residual obtained with 21 parameters (noted $\log(J_{21})$). We then obtain a regression line whose equation is given by

16

$y = 1.091x - 0.064$. Hence $\dfrac{J_{17}}{J_{21}} = 0.938\, J_{21}^{0.091}$ and this points out that when the number of iterations is big, the gap between J_{17} and J_{21} is big too (J_{17} is much smaller than J_{21}).

The problem is: *how to know the number of parameters with which we must work to well approximate the shape?* Indeed, if we work with too few parameters we cannot detect a non-trivial shape and if we work with too many parameters, degeneracy of the functional leads problems. From now, we present some numerical illustrations.

4.3 An *adaptive method*

A solution which seems to be efficient is to use an *adaptive method*. It consists in increasing gradually the number of parameters during the algorithm to a fixed final number of parameters. For example, if we want to work with twenty-one parameters, we begin by working with two parameters during five iterations, then with three parameters (we add the radius) during five more iterations, and then we add two search parameters every fifteen iterations.

We also adapt the number of discretization points for the interior boundary (we conserve the same for the exterior boundary). We fix a minimum number of discretization points (here 40). Then, when we consider the perturbation directions associated to $\cos(k\theta)$ and $\sin(k\theta)$, we discretize the interior boundary using $N_{int} = 9 * k$ points. This method permits to discretize half of a period using five points, which seems suitable.

The algorithm is the same than Algorithm 1 described above. However, the step 6. is replaced by

$$\omega_{i+1}(1:m) = \omega_i(1:m) - \alpha_i \nabla J_{KV}(\omega_i)(1:m),$$

where $\omega_i(1:m)$ represents the m first coefficients parametrizing the shape ω_i (the same notation holds for $\nabla J_{KV}(\omega_i)(1:m)$). The number m grows to the fixed final number of parameters following the procedure described previously. This process permits to avoid the oscillations of the boundary as what is shown in Figure 4. Indeed, we saw in Figure 3
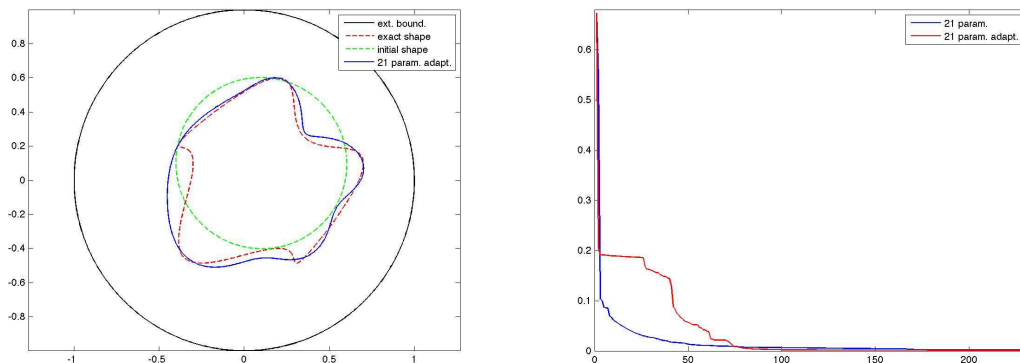

Figure 4: Reconstruction of ω_2^* using the *adaptive method* with 21 parameters

that if we work with twenty-one parameters, oscillations appear but we see in Figure 4 that it is not the case using this *adaptive method*. We can notice that this *adaptive method* leads to steps in the evolution of the residual. Hence this *adaptive method* seems to be efficient and permits to reconstruct the obstacle removing the oscillations due to the *high frequencies*.

4.4 Detecting objects with corners

In order to test the performances of our algorithm and of our *adaptive method*, we want now to detect more complicated obstacles and particularly, we wonder if it is effective to reconstruct objects containing straight lines and corners.

The first objective is then to detect the square ω_3^* whose vertices are the points $(-0.55, -0.55)$, $(0.55, -0.55)$, $(0.55, 0.55)$ and $(-0.55, 0.55)$. We see in Figure 5 that this
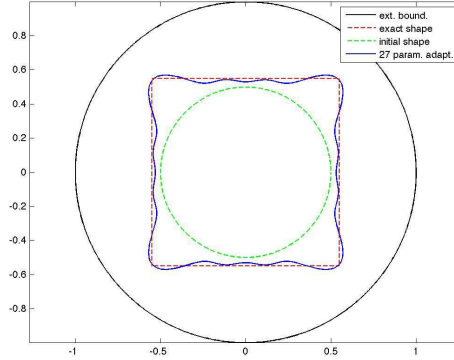

Figure 5: Reconstruction of ω_3^* using the *adaptive method* with 27 parameters

reconstruction is quite efficient. However, if we want to reconstruct a smaller object, the results are significantly worse. Indeed, in Figure 6, we reconstruct the square ω_4^* whose
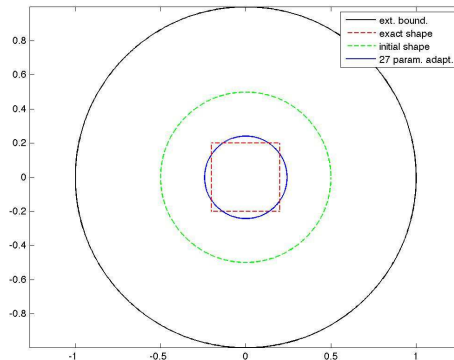

Figure 6: Reconstruction of ω_4^* using the *adaptive method* with 27 parameters

vertices are the points $(-0.2, -0.2)$, $(0.2, -0.2)$, $(0.2, 0.2)$ and $(-0.2, 0.2)$. We see that the detection is not good. This phenomenon concerning the size of the object was underlined using the explicit calculus of the shape Hessian in Table 1 (in Example 8).

Thus, the parametrization method coupling with our *adaptive method* seems to be efficient to reconstruct obstacles, even if the shapes are not trivial. However, the regularizing behavior complicate the detection of small objects or of distant parts of the measurement domain.

4.5 Influence of the size of the domain where measurements are made

Let us consider the influence of the size of O, the part of the boundary where the measurements are assumed to be made. We now restrict the domain O to some part of $\partial\Omega$. We precise that we use here exactly the same algorithm and the same parameters and data that the ones used in Section 4.3. In particular we use the previously described *adaptive method* and we want to reconstruct the object ω_2^* which is given by (4.1).

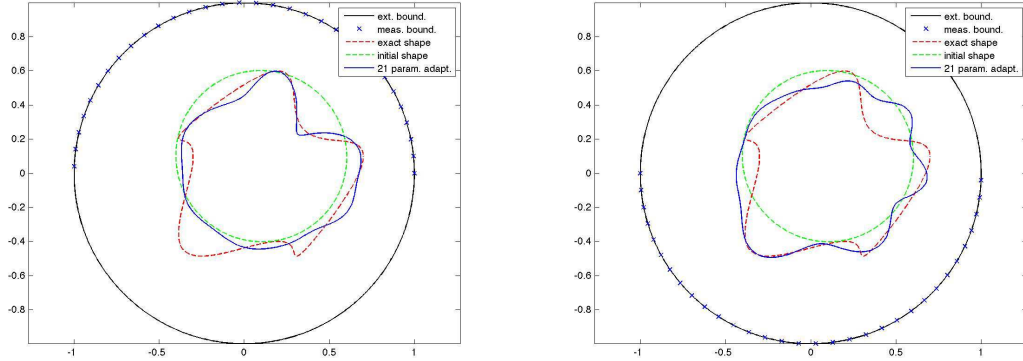In Figure 7, we make the measurement only on a semicircle. On the left of Figure 7,

Figure 7: Reconstruction of ω_2^* using the *adaptive method* with 21 parameters restricting the measurement domain (O is a half of $\partial\Omega$)

O is the upper semicircle. As we could expect, the reconstruction of the object ω_2^* is less efficient than in the case $O = \partial\Omega$ (see Figure 4). In particular, the bottom of the obstacle (*i.e.* the part exposed to the part of the exterior boundary where we do not make the measurement) is poorly detected. We precise that here, we do not obtain a residual $\varepsilon \approx 10^{-3}$ as in the case $O = \partial\Omega$ but only $\varepsilon \approx 6.8 \cdot 10^{-3}$. On the right of Figure 7, O is the lower semicircle. We obtain similar results. As we expected, we see that in this case only the bottom of the obstacle is well detected.

In Figure 8, O is the right superior quart-circle. Here again, the reconstruction is less
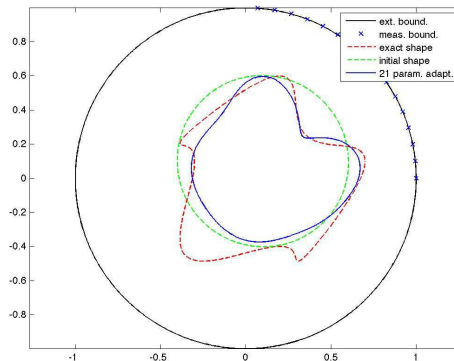

Figure 8: Reconstruction of ω_2^* using the *adaptive method* with 21 parameters restricting the measurement domain (O is a quarter of $\partial\Omega$)

efficient than in the case $O = \partial\Omega$ and even in the previous case $O = \frac{1}{2}\partial\Omega$. We can notice

again that only the part exposed to the measurement domain O is well determined. Here, we only obtain a residual $\varepsilon \approx 8.4 \cdot 10^{-3}$.

These two simulations emphasize an intuitive idea: the more the measurement domain $O \subset \partial\Omega$ is small, the more it is difficult to well reconstruct the object ω.

4.6 Detecting more than one object

Theoretically, besides the regularity assumptions, the main assumption is that $\Omega \backslash \overline{\omega}$ is connected. This assumption does not exclude the case of two or more inclusions in Ω. Thus, we want now to detect numerically two objects: a square ω_5^* whose vertices are the points $(-0.6, 0.1)$, $(-0.1, 0.1)$, $(-0.1, 0.6)$ and $(-0.6, 0.6)$ and a circle ω_6^* centered at $(0.35, -0.35)$ with radius 0.35. Here again we use the *adaptive method* described in Section 4.3. Since the computation is significantly longer than the one with only one object, we stop the experiment when the residual is $\varepsilon \approx 1.5\mathrm{e}{-02}$. We then obtain Figure 9.
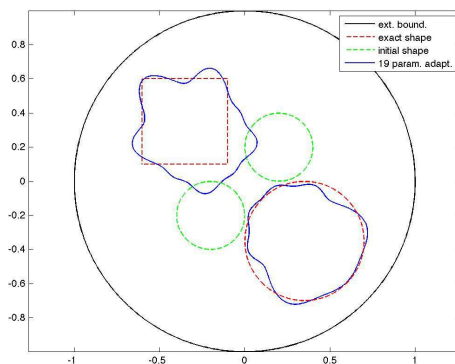

Figure 9: Reconstruction of ω_5^* and ω_6^* using the *adaptive method* with 19 parameters

This result is satisfying and we can hope that it would be more efficient if we increase the accuracy of the computation (using a better finite elements discretization for example) and/or if we increase the computation time. Notice that the non-smooth square is not as-well reconstructed as the circle: this is caused by the polar representation we used.

Notice an important remark. The parametric method that we adopted here to detect the objects does not permit to modify the topology of the object ω. Thus, in order to detect two or more inclusions, we have to know how many objects are included in Ω. A solution could be to initialize the algorithm using the notion of *topological gradient* (see for example [11], [19] or [29]) which could give us the number of inclusions and their rough location, providing initial shapes for our optimization method.

5 Conclusion

We have partially reconstructed an obstacle immersed in a fluid by minimizing the Kohn-Vogelius functional. The Kohn-Vogelius approach proposed here is not the classical one and permits to make the measurement only on a part of the exterior boundary and not on the whole exterior boundary. We have used shape optimization methods to compute the gradient and to motivate the use of a parametric model to solve numerically the inverse problem. Indeed, this problem is severely ill-posed. In order to highlight the exponentially ill-posedness of our problem, we have computed explicitly the shape Hessian matrix in a

concentric annulus. We have then compared our Stokes case with the Laplacian situation and have concluded that the two cases are as ill-posed. The numerical simulations made in the bi-dimensional case were effective but oscillations appeared when we worked with *high frequencies.* In order to remove these oscillations, the *adaptive method* that we proposed seems to be efficient.

There is still some room for improvement principally concerning the numerical issues. Our algorithm permits to reconstruct more than one object if we know how many objects are included in the domain. The use of the notion of *topological gradient* (see for example [11], [19] or [29]) could permit to give us the number of inclusions and their rough location, providing initial shapes for our optimization method.

A   Some results on the Stokes problem with mixed conditions

We recall classical results about the Stokes problem with mixed boundary conditions: a theorem of existence and uniqueness of the solution and a local regularity result.

In all this appendix, we note C a generic positive constant, only depending on the geometry of the domain and on the dimension, which may change from line to line.

First, let us introduce some notations: for Ω an open set of $\mathbb{R}^N$ ($N \in \mathbb{N}^*$), an open subset $\omega \subset\subset \Omega$ and an open subset $O \subset \partial\Omega$ of the exterior boundary, we define

$$\boldsymbol{V}_O(\Omega\backslash\overline{\omega}) := \left\{ \boldsymbol{u} \in \mathbf{H}^1(\Omega\backslash\overline{\omega}); \ \operatorname{div}\boldsymbol{u} = 0 \text{ in } \Omega\backslash\overline{\omega}, \ \boldsymbol{u} = \boldsymbol{0} \text{ on } \partial\omega \cup (\partial\Omega\backslash\overline{O}) \right\}.$$

Moreover, we denote respectively by $\langle \cdot, \cdot \rangle_{\Omega\backslash\overline{\omega}}$ and $\langle \cdot, \cdot \rangle_{\partial\Omega}$ (or $\langle \cdot, \cdot \rangle_{\partial\omega}$) the duality product between $\left[\mathbf{H}^1(\Omega\backslash\overline{\omega})\right]'$ and $\mathbf{H}^1(\Omega\backslash\overline{\omega})$ and the duality product between $\mathbf{H}^{-1/2}(\partial\Omega)$ and $\mathbf{H}^{1/2}(\partial\Omega)$.

Theorem 11 (Existence and uniqueness of the solution). *Let Ω be a bounded Lipschitz open set of $\mathbb{R}^N$ ($N \in \mathbb{N}^*$) and let $\omega \subset\subset \Omega$ be a Lipschitz open subset of Ω such that $\Omega\backslash\overline{\omega}$ is connected. Let O be an open subset of the exterior boundary $\partial\Omega$ and $\nu > 0$. Let*

$$(\boldsymbol{f}, g, \boldsymbol{h_O}, \boldsymbol{h_{ext}}, \boldsymbol{h_{int}}) \in \left[\mathbf{H}^1(\Omega\backslash\overline{\omega})\right]' \times \mathrm{L}^2(\Omega\backslash\overline{\omega}) \times \mathbf{H}^{-1/2}(O) \times \mathbf{H}^{1/2}(\partial\Omega\backslash\overline{O}) \times \mathbf{H}^{1/2}(\partial\omega).$$

Then, the problem

$$\begin{cases} -\nu\Delta\boldsymbol{u} + \nabla p &= \boldsymbol{f} & \text{in } \Omega\backslash\overline{\omega} \\ \operatorname{div}\boldsymbol{u} &= g & \text{in } \Omega\backslash\overline{\omega} \\ -\nu\partial_{\mathbf{n}}\boldsymbol{u} + p\mathbf{n} &= \boldsymbol{h_O} & \text{on } O \\ \boldsymbol{u} &= \boldsymbol{h_{ext}} & \text{on } \partial\Omega\backslash\overline{O} \\ \boldsymbol{u} &= \boldsymbol{h_{int}} & \text{on } \partial\omega \end{cases} \tag{A.1}$$

admits a unique solution $(\boldsymbol{u}, p) \in \mathbf{H}^1(\Omega\backslash\overline{\omega}) \times \mathrm{L}^2(\Omega\backslash\overline{\omega})$ and the following estimate holds:

$$\|\boldsymbol{u}\|_{\mathbf{H}^1(\Omega\backslash\overline{\omega})} + \|p\|_{\mathrm{L}^2(\Omega\backslash\overline{\omega})} \leq C\Big(\|\boldsymbol{f}\|_{[\mathbf{H}^1(\Omega\backslash\overline{\omega})]'} + \|g\|_{\mathrm{L}^2(\Omega\backslash\overline{\omega})}$$
$$+ \|\boldsymbol{h_O}\|_{\mathbf{H}^{-1/2}(O)} + \|\boldsymbol{h_{ext}}\|_{\mathbf{H}^{1/2}(\partial\Omega\backslash\overline{O})} + \|\boldsymbol{h_{int}}\|_{\mathbf{H}^{1/2}(\partial\omega)} \Big).$$

Proof. Step 1: existence and uniqueness. Let us begin by studying the case of null divergence. According to [7, Lemma 3.3], consider $\boldsymbol{H} \in \mathbf{H}^1(\Omega\backslash\overline{\omega})$ such that $\operatorname{div}\boldsymbol{H} = 0$, $\boldsymbol{H} = \boldsymbol{h_{int}}$ on $\partial\omega$, $\boldsymbol{H} = \boldsymbol{h_{ext}}$ on $\partial\Omega\backslash\overline{O}$ such that $\int_{\partial\Omega\cup\partial\omega}\boldsymbol{H}\cdot\mathbf{n} = 0$ and satisfying

$$\|\boldsymbol{H}\|_{\mathbf{H}^1(\Omega\backslash\overline{\omega})} \leq C\left(\|\boldsymbol{h_{int}}\|_{\mathbf{H}^{1/2}(\partial\omega)} + \|\boldsymbol{h_{ext}}\|_{\mathbf{H}^{1/2}(\partial\Omega\backslash\overline{O})}\right). \tag{A.2}$$

Then the couple $(\boldsymbol{U} := \boldsymbol{u} - \boldsymbol{H}, p) \in \mathbf{H}^1(\Omega\backslash\overline{\omega}) \times \mathrm{L}^2(\Omega\backslash\overline{\omega})$ satisfies

$$\begin{cases} -\nu\Delta\boldsymbol{U} + \nabla p &= \boldsymbol{f} + \nu\Delta\boldsymbol{H} & \text{in } \Omega\backslash\overline{\omega} \\ \operatorname{div}\boldsymbol{U} &= 0 & \text{in } \Omega\backslash\overline{\omega} \\ -\nu\partial_{\mathbf{n}}\boldsymbol{U} + p\mathbf{n} &= \boldsymbol{h_{ext}} + \nu\partial_{\mathbf{n}}\boldsymbol{H} & \text{on } O \\ \boldsymbol{U} &= \boldsymbol{0} & \text{on } \partial\Omega\backslash\overline{O} \\ \boldsymbol{U} &= \boldsymbol{0} & \text{on } \partial\omega. \end{cases}$$

According to Lax-Milgram's theorem, there exists a unique $\boldsymbol{U} \in \boldsymbol{V}_O(\Omega\backslash\overline{\omega})$ such that for all $\boldsymbol{v} \in \boldsymbol{V}_O(\Omega\backslash\overline{\omega})$

$$\nu\int_{\Omega\backslash\overline{\omega}}\nabla\boldsymbol{U} : \nabla\boldsymbol{v} = \langle\boldsymbol{f}, \boldsymbol{v}\rangle_{\Omega\backslash\overline{\omega}} - \nu\int_{\Omega\backslash\overline{\omega}}\nabla\boldsymbol{H} : \nabla\boldsymbol{v} - \langle\boldsymbol{h_O} + \nu\partial_{\mathbf{n}}\boldsymbol{H}, \boldsymbol{v}\rangle_O \tag{A.3}$$

and we have, using (A.2),

$$\|\boldsymbol{U}\|_{\mathbf{H}^1(\Omega\backslash\overline{\omega})} \leq C\left(\|\boldsymbol{f}\|_{[\mathbf{H}^1(\Omega\backslash\overline{\omega})]'} + \|\boldsymbol{h_{int}}\|_{\mathbf{H}^{1/2}(\partial\omega)} + \|\boldsymbol{h_{ext}}\|_{\mathbf{H}^{1/2}(\partial\Omega\backslash\overline{O})} + \|\boldsymbol{h_O}\|_{\mathbf{H}^{-1/2}(O)}\right). \tag{A.4}$$

In particular (A.3) is true for all $\boldsymbol{v} \in \boldsymbol{V}_O(\Omega\backslash\overline{\omega}) \cap \mathbf{H}_0^1(\Omega\backslash\overline{\omega})$. Then using De Rham's theorem (see for example [6, Lemma 2.7]), there exists $p \in \mathrm{L}^2(\Omega\backslash\overline{\omega})$, up to an additive constant, such that for all $\boldsymbol{v} \in \mathbf{H}_0^1(\Omega\backslash\overline{\omega})$

$$\nu\int_{\Omega\backslash\overline{\omega}}\nabla\boldsymbol{U} : \nabla\boldsymbol{v} - \int_{\Omega\backslash\overline{\omega}}p\operatorname{div}\boldsymbol{v} = \left\langle\boldsymbol{f}|_{\mathbf{H}_0^1(\Omega\backslash\overline{\omega})}, \boldsymbol{v}\right\rangle_{\mathbf{H}^{-1}(\Omega\backslash\overline{\omega}), \mathbf{H}_0^1(\Omega\backslash\overline{\omega})} - \nu\int_{\Omega\backslash\overline{\omega}}\nabla\boldsymbol{H} : \nabla\boldsymbol{v}. \tag{A.5}$$

According to [7, Lemma 3.3] or [18, Theorem 3.2], we define $\boldsymbol{\varphi}_N \in \mathbf{H}^1(\Omega\backslash\overline{\omega})$ such that $\operatorname{div}\boldsymbol{\varphi}_N = 1$ in $\Omega\backslash\overline{\omega}$, $\boldsymbol{\varphi}_N = \boldsymbol{0}$ on $\partial\Omega\backslash\overline{O}$ and $\boldsymbol{\varphi}_N = \boldsymbol{0}$ on $\partial\omega$ with $\int_O\boldsymbol{\varphi}_N\cdot\mathbf{n} \neq 0$. Let $\boldsymbol{v} \in \mathbf{H}^1(\Omega\backslash\overline{\omega})$ such that $\boldsymbol{v} = \boldsymbol{0}$ on $\partial\Omega\backslash\overline{O}$, $\boldsymbol{v} = \boldsymbol{0}$ on $\partial\omega$ and define

$$c_b(\boldsymbol{v}) = \frac{1}{\int_{\partial(\Omega\backslash\omega)}\boldsymbol{\varphi}_N\cdot\mathbf{n}}\int_{\partial(\Omega\backslash\overline{\omega})}\boldsymbol{v}\cdot\mathbf{n}.$$

Using again [7, Lemma 3.3] or [18, Theorem 3.2], we define $\boldsymbol{v}_2 \in \boldsymbol{V}_O(\Omega\backslash\overline{\omega})$ in such a way that $\boldsymbol{v} = \boldsymbol{v}_1 + \boldsymbol{v}_2 + c_b(\boldsymbol{v})\boldsymbol{\varphi}_N$, where $\boldsymbol{v}_1 \in \mathbf{H}_0^1(\Omega\backslash\overline{\omega})$ satisfies the following equality: $\operatorname{div}\boldsymbol{v}_1 = \operatorname{div}(\boldsymbol{v} - c_b(\boldsymbol{v})\boldsymbol{\varphi}_N)$. Then, using (A.3) and (A.5), we obtain

$$\int_{\Omega\backslash\overline{\omega}}\nu\nabla\boldsymbol{U} : \nabla\boldsymbol{v} - \int_{\Omega\backslash\overline{\omega}}p\operatorname{div}\boldsymbol{v} = \langle\boldsymbol{f}, \boldsymbol{v}\rangle_{\Omega\backslash\overline{\omega}} - \nu\int_{\Omega\backslash\overline{\omega}}\nabla\boldsymbol{H} : \nabla\boldsymbol{v}$$

$$- \langle\boldsymbol{h_O} + \nu\partial_{\mathbf{n}}\boldsymbol{H}, \boldsymbol{v}\rangle_O + \int_{\Omega\backslash\overline{\omega}}\nu\nabla\boldsymbol{U} : \nabla(c_b(\boldsymbol{v})\boldsymbol{\varphi}_N) - \int_{\Omega\backslash\overline{\omega}}p\operatorname{div}(c_b(\boldsymbol{v})\boldsymbol{\varphi}_N)$$

$$- \langle\boldsymbol{f}, c_b(\boldsymbol{v})\boldsymbol{\varphi}_N\rangle_{\Omega\backslash\overline{\omega}} + \nu\int_{\Omega\backslash\overline{\omega}}\nabla\boldsymbol{H} : \nabla(c_b(\boldsymbol{v})\boldsymbol{\varphi}_N) + \langle\boldsymbol{h_O} + \nu\partial_{\mathbf{n}}\boldsymbol{H}, c_b(\boldsymbol{v})\boldsymbol{\varphi}_N\rangle_O.$$

22

Therefore, choosing the additive constant for p such that

$$\int_{\Omega\setminus\overline{\omega}} p = \nu \int_{\Omega\setminus\overline{\omega}} \nabla \boldsymbol{U} : \nabla \boldsymbol{\varphi}_N$$
$$- \langle \boldsymbol{f}, c_b(\boldsymbol{v})\boldsymbol{\varphi}_N \rangle_{\Omega\setminus\overline{\omega}} + \nu \int_{\Omega\setminus\overline{\omega}} \nabla \boldsymbol{H} : \nabla \boldsymbol{\varphi}_N + \langle \boldsymbol{h_O} + \nu \partial_{\mathbf{n}} \boldsymbol{H}, c_b(\boldsymbol{v})\boldsymbol{\varphi}_N \rangle_O \,,$$

we prove that there exists a unique pair $(\boldsymbol{U}, p) \in \boldsymbol{V}_O(\Omega\setminus\overline{\omega}) \times \mathrm{L}^2(\Omega\setminus\overline{\omega})$ such that for all $\boldsymbol{v} \in \mathbf{H}^1(\Omega\setminus\overline{\omega})$ with $\boldsymbol{v} = \mathbf{0}$ on $\partial\Omega\setminus\overline{O}$ and $\boldsymbol{v} = \mathbf{0}$ on $\partial\omega$,

$$\int_{\Omega\setminus\overline{\omega}} \nu \nabla \boldsymbol{U} : \nabla \boldsymbol{v} - \int_{\Omega\setminus\overline{\omega}} p \operatorname{div} \boldsymbol{v} = \langle \boldsymbol{f}, \boldsymbol{v} \rangle_{\Omega\setminus\overline{\omega}} - \nu \int_{\Omega\setminus\overline{\omega}} \nabla \boldsymbol{H} : \nabla \boldsymbol{v} - \langle \boldsymbol{h_O} + \nu \partial_{\mathbf{n}} \boldsymbol{H}, \boldsymbol{v} \rangle_O \,. \quad \text{(A.6)}$$

Step 2: estimate. Let $\boldsymbol{v} := \widetilde{\boldsymbol{v}} + c(p)\boldsymbol{\varphi}_N$, where

$$c(p) := \frac{1}{|\Omega\setminus\overline{\omega}|} \int_{\Omega\setminus\overline{\omega}} p$$

and $\widetilde{\boldsymbol{v}} \in \mathbf{H}^1_0(\Omega\setminus\overline{\omega})$ is such that $\operatorname{div} \widetilde{\boldsymbol{v}} = p - c(p)$ and $\|\widetilde{\boldsymbol{v}}\|_{\mathbf{H}^1_0(\Omega\setminus\overline{\omega})} \leq C \|p\|_{\mathrm{L}^2(\Omega\setminus\overline{\omega})}$ (see [7, Lemma 3.3]). Using $\boldsymbol{v}$ in (A.6), and according to (A.4), we obtain

$$\|\boldsymbol{U}\|_{\mathbf{H}^1(\Omega\setminus\overline{\omega})} + \|p\|_{\mathrm{L}^2(\Omega\setminus\overline{\omega})}$$
$$\leq C \left(\|\boldsymbol{f}\|_{[\mathbf{H}^1(\Omega\setminus\overline{\omega})]'} + \|\boldsymbol{h_{int}}\|_{\mathbf{H}^{1/2}(\partial\omega)} + \|\boldsymbol{h_{ext}}\|_{\mathbf{H}^{1/2}(\partial\Omega\setminus\overline{O})} + \|\boldsymbol{h_O}\|_{\mathbf{H}^{-1/2}(O)} \right)$$

and hence

$$\|\boldsymbol{u}\|_{\mathbf{H}^1(\Omega\setminus\overline{\omega})} + \|p\|_{\mathrm{L}^2(\Omega\setminus\overline{\omega})}$$
$$\leq C \left(\|\boldsymbol{f}\|_{[\mathbf{H}^1(\Omega\setminus\overline{\omega})]'} + \|\boldsymbol{h_{int}}\|_{\mathbf{H}^{1/2}(\partial\omega)} + \|\boldsymbol{h_{ext}}\|_{\mathbf{H}^{1/2}(\partial\Omega\setminus\overline{O})} + \|\boldsymbol{h_O}\|_{\mathbf{H}^{-1/2}(O)} \right)$$

Step 3: case $g \neq 0$. The first part of the theorem is proved for $g = 0$. The case $g \neq 0$ is obtained by a lifting argument. Let us define

$$\boldsymbol{u_g} := \widetilde{\boldsymbol{u_g}} + c(g)\boldsymbol{\varphi_N} - \frac{1}{|\Omega\setminus\overline{\omega}|} \int_{\Omega\setminus\overline{\omega}} (\widetilde{\boldsymbol{u_g}} + c(g)\boldsymbol{\varphi_N}) \in \mathbf{H}^1(\Omega\setminus\overline{\omega}),$$

where

$$c(g) := \frac{1}{|\Omega\setminus\overline{\omega}|} \int_{\Omega\setminus\overline{\omega}} g$$

and where, according to [18, Theorem 3.2] or [7, Lemma 3.3], $\widetilde{\boldsymbol{u_g}} \in \mathbf{H}^1_0(\Omega\setminus\overline{\omega})$ is such that $\operatorname{div} \widetilde{\boldsymbol{u_g}} = g - c(g)$ and $\|\widetilde{\boldsymbol{u_g}}\|_{\mathbf{H}^1_0(\Omega\setminus\overline{\omega})} \leq C\|g\|_{\mathrm{L}^2(\Omega\setminus\overline{\omega})}$. Thus $\boldsymbol{u_g}$ is such that

$$\int_{\Omega\setminus\overline{\omega}} \boldsymbol{u_g} = \mathbf{0}, \quad \operatorname{div} \boldsymbol{u_g} = g \text{ in } \Omega\setminus\overline{\omega} \quad \text{and} \quad \|\boldsymbol{u_g}\|_{\mathbf{H}^1(\Omega\setminus\overline{\omega})} \leq C\|g\|_{\mathrm{L}^2(\Omega\setminus\overline{\omega})}.$$

Thus, defining $\boldsymbol{u_0} := \boldsymbol{u} - \boldsymbol{u_g}$ and

$$\widetilde{\boldsymbol{f}} : \boldsymbol{v} \in \mathbf{H}^1(\Omega\setminus\overline{\omega}) \mapsto \langle \boldsymbol{f}, \boldsymbol{v} \rangle_{\Omega\setminus\overline{\omega}} - \nu \int_{\Omega\setminus\overline{\omega}} \nabla \boldsymbol{H} : \nabla \boldsymbol{v} - \nu \int_{\Omega\setminus\overline{\omega}} \nabla \boldsymbol{u_g} : \nabla \boldsymbol{v},$$

the problem (A.1) is equivalent to

$$\begin{cases} \text{Find } (\boldsymbol{u_0}, p) \in \boldsymbol{V}_O(\Omega\setminus\overline{\omega}) \times \mathrm{L}^2(\Omega\setminus\overline{\omega}) \text{ such that} \\ \displaystyle\int_{\Omega\setminus\overline{\omega}} \nu \nabla \boldsymbol{u_0} : \nabla \boldsymbol{v} - \int_{\Omega\setminus\overline{\omega}} p \operatorname{div} \boldsymbol{v} = \left\langle \widetilde{\boldsymbol{f}}, \boldsymbol{v} \right\rangle_{\Omega\setminus\overline{\omega}} - \langle \boldsymbol{h_O} + \nu \partial_{\mathbf{n}} \boldsymbol{H}, \boldsymbol{v} \rangle_O \\ \forall \boldsymbol{v} \in \mathbf{H}^1(\Omega\setminus\overline{\omega}), \ \boldsymbol{v} = \mathbf{0} \text{ on } \partial\omega, \ \boldsymbol{v} = \mathbf{0} \text{ on } \partial\Omega\setminus\overline{O}. \end{cases}$$

Then we proceed in the same manner as the case $g = 0$. $\qquad\square$

Let us now state and prove a local regularity result on the solution of the Stokes problem with mixed boundary conditions. We first introduce the following notations: for $k, m \in \mathbb{N}$, $k < m$ and for two open sets Ω_1 et Ω_2 such that $\Omega_2 \subset \Omega_1$, we denote by $X^{k,m}(\Omega_1, \Omega_2)$ the space of functions in $\mathbf{H}^k(\Omega_1)$ such that their restriction to Ω_2 belongs to $\mathbf{H}^m(\Omega_2)$. Similarly, we note $X^{*,m}(\Omega_1, \Omega_2)$ the space of functions in $\left[\mathbf{H}^1(\Omega_1)\right]'$ such that their restriction to Ω_2 belongs to $\mathbf{H}^m(\Omega_2)$.

Theorem 12 (Local regularity result). *Let $k \in \mathbb{N}$, $\nu > 0$, Ω a bounded Lipschitz open set of $\mathbb{R}^N$ ($N \in \mathbb{N}^*$) and ω an open set with a $C^{k+1,1}$ boundary such that $\omega \subset\subset \Omega$ and $\Omega \backslash \overline{\omega}$ is connected. Let O be an open subset of the exterior boundary $\partial\Omega$ and $\nu > 0$. Let $\mathcal{C}$ and $\mathcal{C}'$ two smooth open subsets of $\Omega \backslash \overline{\omega}$ such that $\partial\omega \subset \partial\mathcal{C}$, $\partial\omega \subset \partial\mathcal{C}'$, $\overline{\mathcal{C}} \backslash \partial\omega \subset \mathcal{C}'$ and $\overline{\mathcal{C}'} \subset \Omega$. Let*

$$(\boldsymbol{f}, g, \boldsymbol{h_O}, \boldsymbol{h_{ext}}, \boldsymbol{h_{int}})$$
$$\in \mathbf{X}^{*,k}(\Omega \backslash \overline{\omega}, \mathcal{C}') \times \mathrm{X}^{0,k+1}(\Omega \backslash \overline{\omega}, \mathcal{C}') \times \mathbf{H}^{-1/2}(O) \times \mathbf{H}^{1/2}(\partial\Omega \backslash \overline{O}) \times \mathbf{H}^{k+\frac{1}{2}}(\partial\omega).$$

We consider $(\boldsymbol{u}, p) \in \mathbf{H}^1(\Omega \backslash \overline{\omega}) \times \mathrm{L}^2(\Omega \backslash \overline{\omega})$ the solution of the following Stokes problem

$$\left\{ \begin{array}{rcll} -\nu\Delta\boldsymbol{u} + \nabla p & = & \boldsymbol{f} & \text{in } \Omega \backslash \overline{\omega} \\ \operatorname{div}\boldsymbol{u} & = & g & \text{in } \Omega \backslash \overline{\omega} \\ -\nu\partial_{\mathbf{n}}\boldsymbol{u} + p\mathbf{n} & = & \boldsymbol{h_O} & \text{on } O \\ \boldsymbol{u} & = & \boldsymbol{h_{ext}} & \text{on } \partial\Omega \backslash \overline{O} \\ \boldsymbol{u} & = & \boldsymbol{h_{int}} & \text{on } \partial\omega. \end{array} \right. \tag{A.7}$$

Then $(\boldsymbol{u}, p)$ belongs to $\mathbf{H}^{k+2}(\mathcal{C}) \times \mathrm{H}^{k+1}(\mathcal{C})$ and the following estimate holds:

$$\|\boldsymbol{u}\|_{\mathbf{H}^{k+2}(\mathcal{C})} + \|p\|_{\mathrm{H}^{k+1}(\mathcal{C})} \leq C\Big(\|\boldsymbol{f}\|_{\mathbf{X}^{*,k}(\Omega \backslash \overline{\omega}, \mathcal{C}')} + \|g\|_{\mathrm{X}^{0,k+1}(\Omega \backslash \overline{\omega}, \mathcal{C}')}$$
$$+ \|\boldsymbol{h_O}\|_{\mathbf{H}^{-1/2}(O)} + \|\boldsymbol{h_{ext}}\|_{\mathbf{H}^{1/2}(\partial\Omega \backslash \overline{O})} + \|\boldsymbol{h_{int}}\|_{\mathbf{H}^{k+\frac{1}{2}}(\partial\omega)} \Big).$$

Proof. First, let us consider the case $k = 0$. We define $\mathcal{V} = \mathcal{C} \cup \overline{\omega}$, $\mathcal{V}' = \mathcal{C}' \cup \overline{\omega}$ and $\varphi \in C_c^\infty(\Omega)$ such that $0 \leq \varphi \leq 1$, $\varphi \equiv 1$ in $\mathcal{V}$ and $\varphi = 0$ in $\Omega \backslash \mathcal{V}'$. Let

$$(\boldsymbol{u}, p) \in \mathbf{H}^1(\Omega \backslash \overline{\omega}) \times \mathrm{L}^2(\Omega \backslash \overline{\omega})$$

the solution of problem (A.7) given by Theorem 11. Using (A.7) we check

$$\left\{ \begin{array}{rcll} -\nu\Delta(\varphi\boldsymbol{u}) + \nabla(\varphi p) & = & \widetilde{\boldsymbol{f}} & \text{in } \mathcal{C}' \\ \operatorname{div}(\varphi\boldsymbol{u}) & = & \widetilde{g} & \text{in } \mathcal{C}' \\ \varphi\boldsymbol{u} & = & \boldsymbol{0} & \text{on } \partial\mathcal{V}' \\ \varphi\boldsymbol{u} & = & \boldsymbol{h_{int}} & \text{on } \partial\omega, \end{array} \right.$$

where $\widetilde{\boldsymbol{f}} := \varphi\boldsymbol{f} - \nu\boldsymbol{u}\Delta\varphi - 2\nu\nabla\boldsymbol{u}\nabla\varphi + p\nabla\varphi$ belongs to $\mathbf{L}^2(\mathcal{C}')$ and $\widetilde{g} := \varphi g + \boldsymbol{u} \cdot \nabla\varphi$ belongs to $\mathrm{H}^1(\mathcal{C}')$. From the regularity of the solutions of the Stokes equations with Dirichlet boundary conditions (see for example [12] or [18]), $\varphi\boldsymbol{u} \in \mathbf{H}^2(\mathcal{C}')$, $\varphi p \in \mathrm{H}^1(\mathcal{C}')$ and from the expression of $\widetilde{\boldsymbol{f}}$ and $\widetilde{g}$ we obtain

$$\|\varphi\boldsymbol{u}\|_{\mathbf{H}^2(\mathcal{C}')} + \|\varphi p\|_{\mathrm{H}^1(\mathcal{C}')} \leq C\Big(\|\varphi\boldsymbol{f}\|_{\mathbf{L}^2(\mathcal{C}')} + \|\varphi g\|_{\mathrm{H}^1(\mathcal{C}')}$$
$$+ \|\boldsymbol{u}\|_{\mathbf{H}^1(\Omega \backslash \overline{\omega})} + \|p\|_{\mathrm{L}^2(\Omega \backslash \overline{\omega})} + \|\boldsymbol{h_{int}}\|_{\mathbf{H}^{\frac{1}{2}}(\partial\omega)} \Big).$$

Using this inequality and the estimate on $\|\boldsymbol{u}\|_{\mathbf{H}^1(\Omega \backslash \overline{\omega})}$ and $\|p\|_{\mathrm{L}^2(\Omega \backslash \overline{\omega})}$ given by Theorem 11, we obtain the announced estimate for $k = 0$. We then proceed by induction for the cases $k \geq 1$. $\qquad\square$

B   Resolution of the Stokes equations in a concentric annulus

In this section, we solve explicitly some Stokes boundary value problems set in the concentric annulus

$$\Omega_\rho = \{x \in \mathbb{R}^2, \rho < |x| < 1\}.$$

The pair $(\vec{e}_r, \vec{e}_\theta) := \left(\begin{pmatrix} \cos\theta \\ \sin\theta \end{pmatrix}, \begin{pmatrix} -\sin\theta \\ \cos\theta \end{pmatrix} \right)$ represents the polar coordinates system.

In order to simplify the expressions, we here assume $\nu = 1$ and $O = \partial\Omega$. We first use the partial differential equations to derive the special form of the solution, then reduce the resolution of the boundary value problem to some linear system.

B.1   Using the PDE

Noticing that the incompressibility condition $\operatorname{div} \boldsymbol{u} = 0$ implies that the pressure p is harmonic, we pass in polar coordinates (r, θ) in which p can be expanded in Laurent's series. Hence we seek the velocity $\boldsymbol{u}$ and the pressure under the form:

$$\boldsymbol{u}(r, \theta) = \begin{pmatrix} u_r(r, \theta) \\ u_\theta(r, \theta) \end{pmatrix} = \begin{pmatrix} \displaystyle\sum_{n \in \mathbb{Z}} u_{n,r}(r) e^{in\theta} \\ \displaystyle\sum_{n \in \mathbb{Z}} u_{n,\theta}(r) e^{in\theta} \end{pmatrix} \quad \text{and} \quad p(r, \theta) = \sum_{n \in \mathbb{Z}} p_n(r) e^{in\theta},$$

with

$$p_0(r) = \alpha_0 + \beta_0 \ln r \quad \text{and} \quad p_n(r) = \alpha_n r^{|n|} + \beta_n r^{-|n|}, \ n \in \mathbb{Z}^*.$$

We distinguish the case $n = 0$ of the other Fourier modes.

Case $n = 0$.   We are led to solve:

$$u_{0,r}'' + \frac{1}{r} u_{0,r}' - \frac{1}{r^2} u_{0,r} = \frac{\beta_0}{r} \quad \text{and} \quad u_{0,\theta}'' + \frac{1}{r} u_{0,\theta}' - \frac{1}{r^2} u_{0,\theta} = 0,$$

whose solutions are

$$u_{0,r}(r) = A_{0,r} r + \frac{B_{0,r}}{r} + \frac{\beta_0}{2} r \ln r \quad \text{and} \quad u_{0,\theta}(r) = A_{0,\theta} r + \frac{B_{0,\theta}}{r}.$$

The incompressibility condition imposes:

$$u_{0,r}(r) = \frac{B_{0,r}}{r} \quad \text{and} \quad u_{0,\theta}(r) = A_{0,\theta} r + \frac{B_{0,\theta}}{r}.$$

Case $n \neq 0$.   We are led to solve the system:

$$\begin{cases} u_{n,r}'' + \frac{3}{r} u_{n,r}' - \frac{n^2-1}{r^2} u_{n,r} = |n| \left[\alpha_n r^{|n|-1} - \beta_n r^{-|n|-1} \right] \\ u_{n,\theta}'' + \frac{1}{r} u_{n,\theta}' - \frac{n^2+1}{r^2} u_{n,\theta} = in \left[\alpha_n r^{|n|-1} + \beta_n r^{-|n|-1} - 2r^{-2} u_{n,r} \right]. \end{cases}$$

As we have a triangular system, we first determine the radial component $u_{n,r}$. We get after some calculations

$$\begin{cases} u_{n,r}(r) = A_{n,r} r^{n-1} + B_{n,r} r^{-n-1} + \frac{\alpha_n}{8} r^2 - \frac{\beta_n}{2} \ln r & \text{if } n = \pm 1 \\ u_{n,r}(r) = A_{n,r} r^{n-1} + B_{n,r} r^{-n-1} + \frac{|n|}{4} \left[\frac{\alpha_n}{|n|+1} r^{|n|+1} + \frac{\beta_n}{|n|-1} r^{-|n|+1} \right] & \text{else.} \end{cases}$$

25

Then we solve the equation in the angular component and impose the incompressibility condition to get

$$
\begin{cases}
u_{n,\theta}(r) = A_{n,r}\,\mathrm{i}\,r^{n-1} - B_{n,r}\,\mathrm{i}\,r^{-n-1} + \alpha_n\mathrm{i}\left(\dfrac{sg(n)}{2} - \dfrac{n}{8}\right)r^2 \\[2mm]
\hspace{3cm} -\dfrac{\mathrm{i}}{2}\beta_n(sg(n) + n\ln r) \quad \text{if } n = \pm 1, \\[4mm]
u_{n,\theta}(r) = A_{n,r}\,\mathrm{i}\,r^{n-1} - B_{n,r}\,\mathrm{i}\,r^{-n-1} + \alpha_n\mathrm{i}\left(\dfrac{sg(n)}{2} - \dfrac{n}{4(|n|+1)}\right)r^{|n|+1} \\[2mm]
\hspace{3cm} +\beta_n\mathrm{i}\left(-\dfrac{sg(n)}{2} + \dfrac{n}{4(|n|-1)}\right)r^{-|n|+1} \quad \text{else,}
\end{cases}
$$

where $sg(n)$ denotes the sign of n. Since we deal with states taking real values, we have obviously

$$
\begin{aligned}
A_{-n,r} &= \overline{B_{n,r}} \\
\alpha_{-n} &= \overline{\alpha_n} \\
\beta_{-n} &= \overline{\beta_n}.
\end{aligned}
$$

The solution $\boldsymbol{u}$. Noticing $\boldsymbol{u}_n = \begin{pmatrix} u_{n,r} \\ u_{n,\theta} \end{pmatrix}$, we have for $n > 1$

$$
\boldsymbol{u}_n(r) = A_{n,r}r^{n-1}\begin{pmatrix} 1 \\ \mathrm{i} \end{pmatrix} + \frac{B_{n,r}}{r^{n+1}}\begin{pmatrix} 1 \\ -\mathrm{i} \end{pmatrix} + \alpha_n r^{n+1}\begin{pmatrix} \frac{n}{4(1+n)} \\ \frac{n+2}{4(1+n)}\mathrm{i} \end{pmatrix} + \beta_n r^{1-n}\begin{pmatrix} \frac{n}{4(n-1)} \\ \frac{2-n}{4(n-1)}\mathrm{i} \end{pmatrix}
$$

with $p = \displaystyle\sum_{n\in\mathbb{Z}^*}\left(\alpha_n r^{|n|} + \beta_n r^{-|n|}\right) + \alpha_0$. We characterize in the same way the solution for $n \leq 1$.

The normal derivative $\partial_{\mathbf{n}}\boldsymbol{u}$. We easily obtain for $n > 1$

$$
\partial_{\mathbf{n}}\boldsymbol{u}_n(r) = (n-1)A_{n,r}r^{n-2}\begin{pmatrix} 1 \\ \mathrm{i} \end{pmatrix} + (n+1)\frac{B_{n,r}}{r^{n+2}}\begin{pmatrix} -1 \\ \mathrm{i} \end{pmatrix}
$$

$$
+ \alpha_n r^n\begin{pmatrix} \frac{n}{4} \\ \frac{n+2}{4}\mathrm{i} \end{pmatrix} + \beta_n r^{-n}\begin{pmatrix} -\frac{n}{4} \\ \frac{n-2}{4}\mathrm{i} \end{pmatrix} \quad \text{(B.1)}
$$

and we characterize $\partial_{\mathbf{n}}\boldsymbol{u}_n$ in the same way for $n \leq 1$.

The Neumann boundary condition $-\partial_{\mathbf{n}}\boldsymbol{u} + p\mathbf{n}$. We easily obtain for $n > 1$

$$
-\partial_{\mathbf{n}}\boldsymbol{u}_n(r) + p_n\mathbf{n} = A_{n,r}r^{n-2}\begin{pmatrix} 1-n \\ \mathrm{i}(1-n) \end{pmatrix} + \frac{B_{n,r}}{r^{n+2}}\begin{pmatrix} n+1 \\ -\mathrm{i}(n+1) \end{pmatrix}
$$

$$
+ \alpha_n r^n\begin{pmatrix} 1-\frac{n}{4} \\ -\frac{n+2}{4}\mathrm{i} \end{pmatrix} + \beta_n r^{-n}\begin{pmatrix} 1+\frac{n}{4} \\ \frac{2-n}{4}\mathrm{i} \end{pmatrix} \quad \text{(B.2)}
$$

and we characterize $-\partial_{\mathbf{n}}\boldsymbol{u}_n + p_n\mathbf{n}$ in the same way for $n \leq 1$.

B.2 Solving the boundary value problems

In order to compute the shape hessian at Ω_ρ, we have to solve two types of boundary value problem: first a Dirichlet's one then a mixed one with Dirichlet boundary condition on the inner boundary and a Neumann boundary condition on the outer one. We recall that we assume for these computations that $O = \partial\Omega$. Thus Problem (1.5) is now

$$
\begin{cases}
-\nu\Delta\boldsymbol{u_N} + \nabla p_N &=\ \boldsymbol{0} \quad \text{in } \Omega\backslash\overline{\omega} \\
\operatorname{div}\boldsymbol{u_N} &=\ 0 \quad \text{in } \Omega\backslash\overline{\omega} \\
-\nu\partial_{\mathbf{n}}\boldsymbol{u_N} + p_N\mathbf{n} &=\ \boldsymbol{g} \quad \text{on } \partial\Omega \\
\boldsymbol{u_N} &=\ \boldsymbol{0} \quad \text{on } \partial\omega.
\end{cases}
$$

From now, we only focus on the cases $n > 1$. We point out that we will choose boundary data such that all the coefficient will be real valued. Thus

$$
\begin{aligned}
A_{-n,r} &= \overline{B_{n,r}} = B_{n,r} \\
\alpha_{-n} &= \overline{\alpha_n} = \alpha_n \\
\beta_{-n} &= \overline{\beta_n} = \beta_n.
\end{aligned}
$$

The solution $\boldsymbol{u_D}$ of the Dirichlet Stokes system. Let us consider $\boldsymbol{f^{(ext)}} \in \mathbf{L}^2(S^1)$ and $\boldsymbol{f^{(int)}} \in \mathbf{L}^2(\rho S^1)$. One seeks $\boldsymbol{u}$ and p such that

$$
\boldsymbol{u} = \boldsymbol{f^{(ext)}}(\theta) = \begin{pmatrix} f_r^{(ext)}(\theta) \\ f_\theta^{(ext)}(\theta) \end{pmatrix} \quad \text{on } \partial\Omega = S^1
$$

$$
\boldsymbol{u} = \boldsymbol{f^{(int)}}(\theta) = \begin{pmatrix} f_r^{(int)}(\theta) \\ f_\theta^{(int)}(\theta) \end{pmatrix} \quad \text{on } \partial\omega = \rho S^1.
$$

The boundary conditions are expanded in Fourier series:

$$
\begin{aligned}
f_r^{(ext)}(\theta) = \sum_{n\in\mathbb{Z}} f_{n,r}^{(ext)}\mathrm{e}^{\mathrm{i}n\theta} \quad &\text{and} \quad f_\theta^{(ext)}(\theta) = \sum_{n\in\mathbb{Z}} f_{n,\theta}^{(ext)}\mathrm{e}^{\mathrm{i}n\theta}, \\
f_r^{(int)}(\theta) = \sum_{n\in\mathbb{Z}} f_{n,r}^{(int)}\mathrm{e}^{\mathrm{i}n\theta} \quad &\text{and} \quad f_\theta^{(int)}(\theta) = \sum_{n\in\mathbb{Z}} f_{n,\theta}^{(int)}\mathrm{e}^{\mathrm{i}n\theta}.
\end{aligned}
$$

We have to seek the (unique) solution of the following linear system

$$
\begin{cases}
A_{n,r}^D + B_{n,r}^D + \dfrac{n}{4n+4}\alpha_n^D + \dfrac{n}{4n-4}\beta_n^D = f_{n,r}^{(ext)} \\[2mm]
A_{n,r}^D - B_{n,r}^D + \dfrac{n+2}{4n+4}\alpha_n^D + \dfrac{2-n}{4n-4}\beta_n^D = \dfrac{f_{n,\theta}^{(ext)}}{\mathrm{i}} \\[2mm]
\rho^{n-1}A_{n,r}^D + \rho^{-n-1}B_{n,r}^D + \dfrac{n}{4n+4}\rho^{n+1}\alpha_n^D + \dfrac{n}{4n-4}\rho^{1-n}\beta_n^D = f_{n,r}^{(int)} \\[2mm]
\rho^{n-1}A_{n,r}^D - \rho^{-n-1}B_{n,r}^D + \dfrac{n+2}{4n+4}\rho^{n+1}\alpha_n^D + \dfrac{2-n}{4n-4}\rho^{1-n}\beta_n^D = \dfrac{f_{n,\theta}^{(int)}}{\mathrm{i}}.
\end{cases}
$$

We point out that we will choose boundary data such that all the coefficients $A_{n,r}^D$, $B_{n,r}^D$, α_n^D and β_n^D will be real valued. We denote

$$
M_n = (\rho^n - \rho^{-n})^2 - n^2(\rho - \rho^{-1})^2.
$$

Using the fact that

$$
\rho^2 - n^2\rho^{2n} + 2\left(-1 + n^2\right)\rho^{2+2n} - n^2\rho^{4+2n} + \rho^{2+4n} = \rho^2\rho^{2n}M_n,
$$

27

we then get the solution of the linear system:

$$A_{n,r}^D = \frac{n^2(1-\rho^2)+(n+2)(\rho^{-2n}-1)}{2M_n}f_{n,r}^{(ext)} + \frac{n((1-\rho^{-2n})+n^2(1-\rho^2))}{2M_n}\frac{f_{n,\theta}^{(ext)}}{i}$$

$$+\frac{n\rho^{-n}(\rho-\rho^{-1})-\rho(\rho^n-\rho^{-n})}{2M_n}f_{n,r}^{(int)} + \frac{n\rho^{-n}(\rho-\rho^{-1})+(n+2)\rho(\rho^n-\rho^{-n})}{2M_n}\frac{f_{n,\theta}^{(int)}}{i}$$

$$B_{n,r}^D = \frac{n^2(1-\rho^2)+(n-2)(1-\rho^{2n})}{2M_n}f_{n,r}^{(ext)} + \frac{(1-\rho^{2n})+n(\rho^2-1)}{2M_n}\frac{f_{n,\theta}^{(ext)}}{i}$$

$$+\frac{(1-n)\rho^{-n}(\rho^{-1}-\rho)+\rho^{n-1}-\rho^{1-n}}{M_n}f_{n,r}^{(int)} + \frac{n^2\rho^n(\rho-\rho^{-1})+n\rho(\rho^n-\rho^{-n})}{2M_n}\frac{f_{n,\theta}^{(int)}}{i}$$

$$\alpha_n^D = \frac{(1-\rho^{-2n})+(n-2)(1-\rho^{-2})}{M_n}f_{n,r}^{(ext)} + 2(1+n)\frac{n(1-\rho^{-2})-(1-\rho^{-2n})}{M_n}\frac{f_{n,\theta}^{(ext)}}{i}$$

$$+\frac{(n-2)\rho^{-n}(\rho-\rho^{-1})+\rho^{-1}(\rho^n-\rho^{n-1})}{2M_n}f_{n,r}^{(int)}$$

$$+\frac{(1+n)\rho^n(\rho-\rho^{-1})+(\rho^{n+1}-\frac{1}{\rho^{n+1}})}{2M_n}\frac{f_{n,\theta}^{(int)}}{i}$$

$$\beta_n^D = \frac{(n-2)(1-\rho^{-2})+(1-\rho^{2n})}{M_n}f_{n,r}^{(ext)} + \frac{n(1-\rho^{-2})+(1-\rho^{2n})}{M_n}\frac{f_{n,\theta}^{(ext)}}{i}$$

$$+2(1-n)\frac{(1+n)\rho^n(\rho-\rho^{-1})+(\rho^{n+1}-\frac{1}{\rho^{n+1}})}{2M_n}f_{n,r}^{(int)}$$

$$+2(n-1)\frac{n\rho^n(\rho-\rho^{-1})+\rho^{-1}(\rho^n-\rho^{-n})}{M_n}\frac{f_{n,\theta}^{(int)}}{i}.$$

Remark 13. *We quote from Engliš and Peetre that M_n is called an Almansi determinant (see [17]). This arise in connection with the following interpolation problem: try to reconstruct a function f of the type $f(x) = P(x) + e^{\mu x}Q(x)$ where P and Q are poynomials of respective degree m, and n, given its value at $m+n$ points $x_1, x_2, \ldots, x_{m+n}$.*

Remark 14. *To compare the factorization in the case of the Laplacian and the case of the Stokes system, we recall that in the case of the Laplacian, we find a denominator equal to*

$$\rho^{|n|} - \rho^{-|n|} = \rho^{-|n|}(\rho^{2|n|}-1) = \rho^{-|n|}(\rho^{|n|}-1)(\rho^{|n|}+1).$$

In the case of Stokes system, we rewrite the denominator as

$$M_n = \left((\rho^{|n|}-\rho^{-|n|})+|n|(\rho^2-\rho^{-2})\right)\left((\rho^{|n|}-\rho^{-|n|})-|n|(\rho^2-\rho^{-2})\right).$$

Application to our case for u_D. We get

$$\begin{pmatrix} A_{n,r}^D \\ B_{n,r}^D \\ \alpha_n^D \\ \beta_n^D \end{pmatrix} = \begin{pmatrix} \frac{n^2(1-\rho^2)+(n+2)(\rho^{-2n}-1)}{2M_n} & \frac{n((1-\rho^{-2n})+n^2(1-\rho^2))}{2M_n} \\ \frac{n^2(1-\rho^2)+(n-2)(1-\rho^{2n})}{2M_n} & \frac{(1-\rho^{2n})+n(\rho^2-1)}{2M_n} \\ \frac{(1-\rho^{-2n})+(n-2)(1-\rho^{-2})}{M_n} & \frac{n(1-\rho^{-2})-(1-\rho^{-2n})}{M_n} \\ \frac{(n-2)(1-\rho^{-2})+(1-\rho^{2n})}{M_n} & 2(1-n)\frac{n(1-\rho^{-2})+(1-\rho^{2n})}{M_n} \end{pmatrix} \begin{pmatrix} f_{n,r} \\ \frac{f_{n,\theta}}{i} \end{pmatrix}.$$

28

We choose $\boldsymbol{f^{(ext)}}(\theta) = \boldsymbol{f}(\theta) = \cos(n\theta)\,\vec{e}_r$, $n > 1$ and $\boldsymbol{f^{(int)}} = \boldsymbol{0}$. Hence $f_{n,r} = \dfrac{1}{2}$, $f_{n,\theta} = 0$ and

$$
\begin{pmatrix} A_{n,r}^D \\ B_{n,r}^D \\ \alpha_n^D \\ \beta_n^D \end{pmatrix} = \frac{1}{2} \begin{pmatrix} \frac{n^2(1-\rho^2)+(n+2)(\rho^{-2n}-1)}{2M_n} \\ \frac{n^2(1-\rho^2)+(n-2)(1-\rho^{2n})}{2M_n} \\ \frac{(1-\rho^{-2n})+(n-2)(1-\rho^{-2})}{M_n} \\ \frac{(n-2)(1-\rho^{-2})+(1-\rho^{2n})}{M_n} \end{pmatrix}.
$$

The solution $\boldsymbol{u_N}$ of the mixed Stokes system. The coefficients are denoted $A_{n,r}^N$, $B_{n,r}^N$ and α_n^N and β_n^N. To fulfill the boundary conditions

$$
-\partial_{\mathbf{n}} \boldsymbol{u_N} + p_N \vec{e}_r = \boldsymbol{g^{(ext)}} \text{ if } |x| = 1 \quad \text{and} \quad \boldsymbol{u_N} = \boldsymbol{g^{(int)}} \text{ if } |x| = \rho,
$$

we have to seek the (unique) solution of the following linear system

$$
\begin{cases}
(1-n)A_{n,r}^N & + & (1+n)B_{n,r}^N & + & \dfrac{4-n}{4}\alpha_n^N & + & \dfrac{4+n}{4}\beta_n^N & = & g_{n,r}^{(ext)} \\[2mm]
(1-n)A_{n,r}^N & - & (1+n)B_{n,r}^N & - & \dfrac{2+n}{4}\alpha_n^N & + & \dfrac{2-n}{4}\beta_n^N & = & \dfrac{g_{n,\theta}^{(ext)}}{i} \\[2mm]
\rho^{n-1}A_{n,r}^N & + & \rho^{-n-1}B_{n,r}^N & + & \rho^{n+1}\dfrac{n}{4n+4}\alpha_n^N & + & \rho^{1-n}\dfrac{n}{4n-4}\beta_n^N & = & g_{n,r}^{(int)} \\[2mm]
\rho^{n-1}A_{n,r}^N & - & B_{n,r}^N\rho^{-n-1} & + & \rho^{n+1}\dfrac{n+2}{4n+4}\alpha_n^N & + & \rho^{1-n}\dfrac{2-n}{4n-4}\beta_n^N & = & \dfrac{g_{n,\theta}^{(int)}}{i}.
\end{cases}
$$
(B.3)

We denote

$$
N_n = 3\rho^2 + (8+n^2)\rho^{2n} - 2(-1+n^2)\rho^{2+2n} + n^2\rho^{4+2n} + 3\rho^{2+4n}
$$

which can be written under the form

$$
N_n = 3(\rho^n - \rho^{-n})^2 + n^2(\rho - \rho^{-1})^2 + 8(1+\rho^{-2}).
$$

The solution of the system corresponding to a general Neumann problem with Dirichlet conditions on the interface is obtained after expanding the inverse of the matrix corresponding to (B.3). We get

$$
\begin{aligned}
A_{n,r}^N \;=\; & -\frac{(n+2)(\rho^{-2n}-1)+n^2(\rho^2-1)+4n}{2(n-1)N_n}g_{n,r}^{(ext)} \\[2mm]
& +\frac{n((1-\rho^{-2n})+n^2(1-\rho^2)}{2N_n}\frac{g_{n,\theta}^{(ext)}}{i} \\[2mm]
& +\frac{3(n+2)\rho(\rho^n-\rho^{-n})+4(n+2)\rho^{-n}(\rho-\rho^{-1})+4(n+4)\rho^{-1-n}}{2N_n}g_{n,r}^{(int)} \\[2mm]
& +\frac{n(n+4)\rho^{-n}(\rho-\rho^{-1})+3n\rho(\rho^n-\rho^{-n})+4(n+2)\rho^{-1-n}}{2N_n}\frac{g_{n,\theta}^{(int)}}{i}
\end{aligned}
$$

$$B_{n,r}^N = -\frac{n^2(1-\rho^2) + (n-2)(\rho^{2n}-1) + 4n}{2(1+n)N_n} g_{n,r}^{(ext)}$$

$$-\frac{(4+n)(\rho^{2n}-1) + n^2(\rho^2-1) + 4(n+2)}{2(1+n)N_n} \frac{g_{n,\theta}^{(ext)}}{i}$$

$$-\frac{(3(n-2)\rho(\rho^{-n}-\rho^n) - (n^2+8)\rho^n(\rho^{-1}-\rho) - 2(n+2)\rho1 + n}{2N_n} g_{n,r}^{(int)}$$

$$+\frac{n^2\rho^n(\rho-\rho^{-1}) - n\rho(\rho^n-\rho^{-n}) - 4n(\rho^{1-n}-\rho^{n-1}) - 4(n+2)\rho^{n-1}}{2N_n} \frac{g_{n,\theta}^{(int)}}{i}$$

$$\alpha_n^N = 2\frac{(2-n)(\rho^{-2}-1) + (\rho^{-2n}-1) + 4}{N_n} g_{n,r}^{(ext)}$$

$$+2\frac{(4+n)(1-\rho^{-2}) + (1-\rho^{-2n}) - 4}{N_n} \frac{g_{n,\theta}^{(ext)}}{i}$$

$$-2(1+n)\frac{(n-1)\rho(\rho^{-n}-\rho^n) + 3\rho(\rho^n-\rho^{-n}) + (4-n)\rho^{1-n}}{N_n} g_{n,r}^{(int)}$$

$$+2(1+n)\frac{(n-1)\rho^{-n}(\rho-\rho^{-1}) + 3(\rho^{n-1}-\rho^{1-n}) + 4\rho^{1-n}}{N_n} \frac{g_{n,\theta}^{(int)}}{i}$$

$$\beta_n^N = \frac{(n+2)(\rho^{-2}-1) + (\rho^{2n}-1) + 4}{N_n} g_{n,r}^{(ext)}$$

$$+\frac{(4-n)(\rho^{-2}-1) + (\rho^{2n}-1) + 2(n-2)}{N_n} \frac{g_{n,\theta}^{(ext)}}{i}$$

$$+2(n-1)\frac{(1+n)\rho^n(\rho-\rho^{-1}) + 3\rho^{-1}(\rho^n-\rho^{-n}) + (n+4)\rho^{n-1}}{N_n} g_{n,r}^{(int)}$$

$$+2(n-1)\frac{n\rho^n(\rho-\rho^{-1}) - \rho^{-1}(\rho^n-\rho^{-n}) - 4\rho-1 - n}{N_n} \frac{g_{n,\theta}^{(int)}}{i}.$$

The Dirichlet-to-Neumnn map. Here, we have to take the Neumann data

$$\boldsymbol{g^{(ext)}} = g_r^{(ext)}\vec{\boldsymbol{e}_r} + g_\theta^{(ext)}\vec{\boldsymbol{e}_\theta}$$

corresponding to the choice of the Dirichlet data $\boldsymbol{f^{(ext)}}$. In order to simplify the expression and to get closer to our case, we assume $\boldsymbol{f^{(int)}} = \boldsymbol{0}$. Omitting the exponent $^{(ext)}$, a straightforward calculation gives

$$g_{n,r} = A_{n,r}^D(1-n) + B_{n,r}^D(1+n) + \frac{4-n}{4}\alpha_n^D + \frac{4+n}{4}\beta_n^D$$

$$g_{n,\theta} = i\left(A_{n,r}^D(1-n) - B_{n,r}^D(1+n) - \frac{2+n}{4}\alpha_n^D + \frac{2-n}{4}\beta_n^D\right),$$

where Fourier coefficients $A_{n,r}^D, B_{n,r}^D, \alpha_n^D$ and β_n^D are given above. The expression with respect to the Fourier coefficients $f_{n,r}$ and $f_{n,\theta}$ is then given by

$$g_{n,r} = -\frac{4(2-n^2)(1-\rho^{-2}) + 2n(\rho^{-2n}-\rho^{2n}) + (\rho^n-\rho^{-n})^2 + n^2(\rho-\rho^{-1})^2}{M_n} f_{n,r}$$

$$+\frac{4n(1-\rho^{-2}) + 2(\rho^{-2n}-\rho^{-2n}) + n^3(\rho-\rho^{-1})^2 + n(\rho^n-\rho^{-n})^2}{M_n} \frac{f_{n,\theta}}{i}$$

and

$$g_{n,\theta} = \mathrm{i}\frac{4n(1-\rho^{-2}) + 2(\rho^{-2n} - \rho^{2n}) + n(\rho^n - \rho^{-n})^2 + n^3(\rho - \rho^{-1})^2}{M_n}f_{n,r}$$
$$- \frac{4n^2(1-\rho^{-2}) + 2n(\rho^{-2n} - \rho^{2n}) + (\rho^{-n} - \rho^n)^2 + n^2(\rho^{-1} - \rho)^2}{M_n}f_{n,\theta}.$$

We illustrate the mapping $(f_{n,r}, f_{n,\theta}) \mapsto (g_{n,r}, g_{n,\theta})$ via the linear transformation

$$\begin{pmatrix} g_{n,r} \\ g_{n,\theta} \end{pmatrix} = \begin{pmatrix} \Delta_{1,1}^{(n)} & \Delta_{1,2}^{(n)} \\ \Delta_{2,1}^{(n)} & \Delta_{2,2}^{(n)} \end{pmatrix} \begin{pmatrix} f_{n,r} \\ f_{n,\theta} \end{pmatrix}$$

where

$$\Delta_{1,1}^{(n)} = -\frac{4(2-n^2)(1-\rho^{-2}) + 2n(\rho^{-2n} - \rho^{2n}) + (\rho^n - \rho^{-n})^2 + n^2(\rho - \rho^{-1})^2}{M_n}$$

$$\Delta_{1,2}^{(n)} = -\mathrm{i}\frac{4n(1-\rho^{-2}) + 2(\rho^{-2n} - \rho^{-2n}) + n^3(\rho - \rho^{-1})^2 + n(\rho^n - \rho^{-n})^2}{M_n}$$

$$\Delta_{2,1}^{(n)} = \overline{\Delta_{1,2}^{(n)}}$$

$$\Delta_{2,2}^{(n)} = -\frac{4n^2(1-\rho^{-2}) + 2n(\rho^{-2n} - \rho^{2n}) + (\rho^{-n} - \rho^n)^2 + n^2(\rho^{-1} - \rho)^2}{M_n}.$$

We can deduce the Dirichlet-to-Neumann map from this representation: in the trigonometric basis it is represented by a block diagonal matrix; its $n-th$ diagonal is given by the matrix $\Delta^{(n)} = (\Delta_{i,j}^{(n)})_{i,j=1,2}$.

Application to our case for u_N.   In our case, with $\boldsymbol{f}^{(ext)}(\theta) = \boldsymbol{f}(\theta) = \cos{(n\theta)}\,\vec{e}_r$, $n > 1$ and $\boldsymbol{f}^{(int)} = \boldsymbol{0}$, we then obtain

$$\begin{cases} g_{n,r} = -\dfrac{4(2-n^2)(1-\rho^{-2}) + 2n(\rho^{-2n} - \rho^{2n}) + (\rho^n - \rho^{-n})^2 + n^2(\rho - \rho^{-1})^2}{M_n}f_{n,r} \\ g_{n,\theta} = \mathrm{i}\dfrac{4n(1-\rho^{-2}) + 2(\rho^{-2n} - \rho^{2n}) + n(\rho^n - \rho^{-n})^2 + n^3(\rho - \rho^{-1})^2}{M_n}f_{n,r}. \end{cases}$$

(B.4)

Hence

$$\begin{pmatrix} A_{n,r}^N \\ B_{n,r}^N \\ \alpha_n^N \\ \beta_n^N \end{pmatrix} = \begin{pmatrix} -\frac{(n+2)(\rho^{-2n}-1)+n^2(\rho^2-1)+4n}{2(n-1)N_n} & \frac{n((1-\rho^{-2n})+n^2(1-\rho^2)}{2N_n} \\ -\frac{n^2(1-\rho^2)+(n-2)(\rho^{2n}-1)+4n}{2(1+n)N_n} & -\frac{(4+n)(\rho^{2n}-1)+n^2(\rho^2-1)+4(n+2)}{2(1+n)N_n} \\ 2\frac{(2-n)(\rho^{-2}-1)+(\rho^{-2n}-1)+4}{N_n} & 2\frac{(4+n)(1-\rho^{-2})+(1-\rho^{-2n})-4}{N_n} \\ \frac{(n+2)(\rho^{-2}-1)+(\rho^{2n}-1)+4}{N_n} & \frac{(4-n)(\rho^{-2}-1)+(\rho^{2n}-1)+2(n-2)}{N_n} \end{pmatrix} \begin{pmatrix} g_{n,r} \\ \frac{g_{n,\theta}}{\mathrm{i}} \end{pmatrix}.$$

B.3   The formulae for the shape derivatives u_D' and u_N'

In this section, we deform the domain via the vector field $\boldsymbol{V} = \cos{k\theta}\,\vec{e}_r$. We then have $V_{\mathrm{n}} = \cos{k\theta}$. Here again, we only focus on the cases $n > 1$.

The formula for the shape derivative u'_D. For $n > 1$, we set

$$
\begin{aligned}
K^D_{n,r} &= A^D_{n,r}(1-n)\rho^{n-2} + \rho^{-n-2}B^D_{n,r}(1+n) - \alpha^D_n \rho^n \frac{n}{4} + \beta^D_n \rho^{-n}\frac{n}{4} \\
L^D_{n,r} &= A^D_{n,r}(1-n)\rho^{n-2} - \rho^{-n-2}B^D_{n,r}(1+n) - \alpha^D_n \rho^n \frac{n+2}{4} + \beta^D_n \rho^{-n}\frac{2-n}{4}
\end{aligned}
\tag{B.5}
$$

the respective Fourier coefficients of $-\partial_{\mathbf{n}}u_D(\rho,\theta)$. As it has been noticed, when $n > 1$, we have

$$
K^D_{-n,r} = \overline{K^D_{n,r}} \quad \text{and} \quad L^D_{-n,r} = -\overline{L^D_{n,r}}.
$$

We will then focus on the coefficients $A^{D'}_{n,r}, B^{D'}_{n,r}, \alpha^{D'}_n$ and $\beta^{D'}_n$ for $n > 1$. Let us point out that the computations give $K^D_{n,r} = 0$. We have (see (B.1))

$$
\begin{aligned}
-\partial_{\mathbf{n}}u_D(\rho,\theta) &= \left(K^D_{n,r}e^{in\theta} + K^D_{-n,r}e^{-in\theta}\right)\vec{e}_r + i\left(L^D_{n,r}e^{in\theta} + L^D_{-n,r}\,e^{-in\theta}\right)\vec{e}_\theta \\
&= i\left(L^D_{n,r}e^{in\theta} - \overline{L^D_{n,r}}\,e^{-in\theta}\right)\vec{e}_\theta
\end{aligned}
$$

and then

$$
-\partial_{\mathbf{n}}u_D\, V_{\mathrm{n}} = i\frac{L^D_{n,r}e^{i(n+k)\theta} + L^D_{-n,r}e^{-i(n+k)\theta}}{2}\vec{e}_\theta + i\frac{L^D_{n,r}e^{i(n-k)\theta} + L^D_{-n,r}e^{-i(n-k)\theta}}{2}\vec{e}_\theta.
$$

Hence

$$
-\partial_{\mathbf{n}}u_D\, V_{\mathrm{n}} = -L^D_{n,r}\Big(\sin\left((n+k)\theta\right) + \sin\left((n-k)\theta\right)\Big)\,\vec{e}_\theta.
$$

We denote

$$
u'_D = \sum_{p \in I_{n,k}} u^{D'}_{p,r}(r)e^{ip\theta}\vec{e}_r + \sum_{p \in I_{n,k}} u^{D'}_{p,\theta}(r)e^{ip\theta}\vec{e}_r,
$$

where $I_{n,k} = \{n+k, n-k, -n-k, -n+k\}$. Let us assume that $-1, 0, 1 \notin I_{n,k}$ (the other cases can be treated similarly). We know that

$$
\begin{cases}
u^{D'}_{p,r}(r) = A^{D'}_{p,r}r^{p-1} + \dfrac{B^{D'}_{p,r}}{r^{p+1}} + \alpha^{D'}_p r^{|p|+1}\dfrac{|p|}{4|p|+4} + \beta^{D'}_p r^{1-|p|}\dfrac{|p|}{4|p|-4} \\[3mm]
u^{D'}_{p,\theta}(r) = i\left(A^{D'}_{p,r}r^{p-1} - \dfrac{B^{D'}_{p,r}}{r^{p+1}} + \alpha_p r^{|p|+1}\left(\dfrac{1}{2}sg(p) - \dfrac{p}{4p+4}\right)\right. \\[3mm]
\qquad\qquad \left. + \beta_p r^{1-|p|}\left(\dfrac{p}{4p-4} - \dfrac{1}{2}sg(p)\right)\right).
\end{cases}
$$

We use the superposition principles: we use the fact that we have to use a linear system associated to a Dirichlet problem and then the coefficients associated to $u^{D'}_{p,r}(r)$ when $p = |n+k|$ and $p = |n-k|$ must satisfy the following linear system

$$
\begin{cases}
A^{D'}_{p,r} &+& B^{D'}_{p,r} &+& \dfrac{p}{4p+4}\alpha^{D'}_p &+& \dfrac{p}{4p-4}\beta^{D'}_p &=& 0 \\[3mm]
A^{D'}_{p,r} &-& B^{D'}_{p,r} &+& \dfrac{p+2}{4p+4}\alpha^{D'}_p &+& \dfrac{2-p}{4p-4}\beta^{D'}_p &=& 0 \\[3mm]
\rho^{p-1}A^{D'}_{p,r} &+& \rho^{-p-1}B^{D'}_{p,r} &+& \dfrac{p}{4p+4}\rho^{p+1}\alpha^{D'}_p &+& \dfrac{p}{4p-4}\rho^{1-p}\beta^{D'}_p &=& K^D_{n,r} \\[3mm]
\rho^{p-1}A^{D'}_{p,r} &-& \rho^{-p-1}B^{D'}_{p,r} &+& \dfrac{p+2}{4p+4}\rho^{p+1}\alpha^{D'}_p &+& \dfrac{2-n}{4p-4}\rho^{1-p}\beta^{D'}_p &=& L^D_{n,r}.
\end{cases}
$$

We remark that the second side of the linear system is independent of k. Once the coefficients are computed, we use (B.2) to get

$$(-\partial_{\mathbf{n}}\boldsymbol{u}'_D + p'_D\mathbf{n})(\rho, \theta) = \left(K^{D'}_{|n+k|,r}\cos(n+k)\theta + K^{D'}_{|n-k|,r}\cos(n-k)\theta\right)\vec{e}_r$$
$$-\left(L^{D'}_{|n+k|,r}\sin(n+k)\theta + L^{D'}_{|n-k|,r}\sin(n-k)\theta\right)\vec{e}_\theta,$$

where

$$K^{D'}_{p,r} = A^{D'}_{p,r}(1-p)\rho^{p-2} + \rho^{-p-2}B^{D'}_{p,r}(1+p) + \alpha^{D'}_p\rho^p\left(1 - \frac{p}{4}\right) + \beta^{D'}_p\rho^{-p}\left(1 + \frac{p}{4}\right)$$
$$L^{D'}_{p,r} = A^{D'}_{p,r}(1-p)\rho^{p-2} - \rho^{-p-2}B^{D'}_{p,r}(1+p) - \alpha^{D'}_p\rho^p\frac{p+2}{4} + \beta^{D'}_p\rho^{-p}\frac{2-p}{4}.$$

The formula for the shape derivative $\boldsymbol{u}'_N$. We adopt the same strategy. We have only to write the corresponding Neumann condition on the exterior boundary (*i.e.* for $|x| = 1$). For $n > 1$, we set

$$K^N_{n,r} = A^N_{n,r}(1-n)\rho^{n-2} + \rho^{-n-2}B^N_{n,r}(1+n) - \alpha^N_n\rho^n\frac{n}{4} + \beta^N_n\rho^{-n}\frac{n}{4}$$
$$L^N_{n,r} = A^N_{n,r}(1-n)\rho^{n-2} - \rho^{-n-2}B^N_{n,r}(1+n) - \alpha^N_n\rho^n\frac{n+2}{4} + \beta^N_n\rho^{-n}\frac{2-n}{4}$$

the respective Fourier coefficients of $-\partial_{\mathbf{n}}\boldsymbol{u}_N(\rho, \theta)$. The computations give

$$K^N_{n,r} = 0$$

and

$$L^N_{n,r} = -2\frac{n(n+2)\rho^{-n}(1-\rho^{-2}) + 4\rho^{-2}(\rho^{-n}-\rho^n) + 2n(n-1)\rho^n(\rho^{-2}-1)}{M_n}f^{(ext)}_{n,r}$$
$$-2\frac{2n^2(\rho^n+\rho^{-n})(\rho^{-2}-1) + 2n(\rho^n-\rho^{-n}) + (1+\rho^{-2})}{M_n}\frac{f^{(ext)}_{n,\theta}}{i}.$$

We solve the system

$$\begin{cases} (1-p)A^{N'}_{p,r} + (1+p)\rho^{-p-2}B^{N'}_{p,r} + \dfrac{4-p}{4}\alpha^{N'}_p + \dfrac{4+p}{4}\beta^{N'}_p = 0 \\[2mm] (1-p)A^{N'}_{p,r} - (1+p)B^{N'}_{p,r} - \dfrac{p+2}{4}\alpha^{N'}_p + \dfrac{2-p}{4}\beta^{N'}_p = 0 \\[2mm] \rho^{p-1}A^{N'}_{p,r} + \rho^{-p-1}B^{N'}_{p,r} + \dfrac{p}{4p+4}\rho^{p+1}\alpha^{N'}_p + \dfrac{p}{4p-4}\rho^{1-p}\beta^{N'}_p = K^N_{n,r} \\[2mm] \rho^{p-1}A^{N'}_{p,r} - \rho^{-p-1}B^{N'}_{p,r} + \dfrac{p+2}{4p+4}\rho^{p+1}\alpha^{N'}_p + \dfrac{2-p}{4p-4}\rho^{1-p}\beta^{N'}_p = L^N_{n,r}. \end{cases}$$

We get

$$A^{N'}_{p,r} = \frac{p(p+4)\rho^{-p}(\rho-\rho^{-1}) + 3p\rho(\rho^p-\rho^{-p}) + 4(p+2)\rho^{-1-p}}{2N_p}L^N_{n,r}$$
$$B^{N'}_{p,r} = \frac{p^2\rho^p(\rho-\rho^{-1}) - p\rho(\rho^p-\rho^{-p}) - 4p(\rho^{1-p}-\rho^{p-1}) - 4(p+2)\rho^{p-1}}{2N_p}L^N_{n,r}$$
$$\alpha^{N'}_p = 2(1+p)\frac{(p-1)\rho^{-p}(\rho-\rho^{-1}) + 3(\rho^{p-1}-\rho^{1-p}) + 4\rho^{1-p}}{N_p}L^N_{n,r}$$
$$\beta^{N'}_p = 2(p-1)\frac{p\rho^p(\rho-\rho^{-1}) - \rho^{-1}(\rho^p-\rho^{-p}) - 4\rho^{-1-p}}{N_p}L^N_{n,r}.$$

We have to compute now

$$(-\partial_{\mathbf{n}}\boldsymbol{u}'_{\boldsymbol{N}} + p'_N \mathbf{n})(\rho, \theta) = \left(K^{N'}_{|n+k|,r} \cos{(n+k)\theta} + K^{N'}_{|n-k|,r} \cos{(n-k)\theta}\right)\vec{\boldsymbol{e}}_r$$
$$-\left(L^{N'}_{|n+k|,r} \sin{(n+k)\theta} + L^{N'}_{|n-k|,r} \sin{(n-k)\theta}\right)\vec{\boldsymbol{e}}_\theta$$

where

$$
\begin{aligned}
K^{N'}_{p,r} &= A^{N'}_{p,r}(1-p)\rho^{p-2} + \rho^{-p-2}B^{N'}_{p,r}(1+p) + \alpha^{N'}_p \rho^n (1 - \frac{p}{4}) + \beta^{N'}_p \rho^{-p}(1 + \frac{p}{4}) \\
L^{N'}_{p,r} &= A^{N'}_{p,r}(1-p)\rho^{p-2} - \rho^{-p-2}B^{N'}_{p,r}(1+p) - \alpha^{N'}_p \rho^p \frac{p+2}{4} + \beta^{N'}_p \rho^{-p}\frac{2-p}{4}.
\end{aligned}
$$

Finally it comes

$$\left(-\partial_{\mathbf{n}}(\boldsymbol{u}'_{\boldsymbol{N}} - \boldsymbol{u}'_{\boldsymbol{D}}) + (p'_N - p'_D)\mathbf{n}\right)(\rho, \theta) = \left(\widetilde{K}_{|n+k|,r} \cos{(n+k)\theta} + \widetilde{K}_{|n-k|,r} \cos{(n-k)\theta}\right)\vec{\boldsymbol{e}}_r$$
$$-\left(\widetilde{L}_{|n+k|,r} \sin{(n+k)\theta} + \widetilde{L}_{|n-k|,r} \sin{(n-k)\theta}\right)\vec{\boldsymbol{e}}_\theta$$

where
$$\widetilde{K}_{p,r} = K^{D'}_{p,r} - K^{N'}_{p,r} \quad \text{and} \quad \widetilde{L}_{p,r} = L^{D'}_{p,r} - L^{N'}_{p,r}. \tag{B.6}$$

References

[1] M. Abdelwahed and M. Hassine. Topological optimization method for a geometric control problem in Stokes flow. *Appl. Numer. Math.*, 59(8):1823–1838, 2009.

[2] L. Afraites, M. Dambrine, K. Eppler, and D. Kateb. Detecting perfectly insulated obstacles by shape optimization techniques of order two. *Discrete Contin. Dyn. Syst. Ser. B*, 8(2):389–416 (electronic), 2007.

[3] L. Afraites, M. Dambrine, and D. Kateb. On second order shape optimization methods for electrical impedance tomography. *SIAM J. Control Optim.*, 47(3):1556–1590, 2008.

[4] C. Alvarez, C. Conca, L. Friz, O. Kavian, and J. H. Ortega. Identification of immersed obstacles via boundary measurements. *Inverse Problems*, 21(5):1531–1552, 2005.

[5] C. J. S. Alves, R. Kress, and A. L. Silvestre. Integral equations for an inverse boundary value problem for the two-dimensional Stokes equations. *J. Inverse Ill-Posed Probl.*, 15(5):461–481, 2007.

[6] C. Amrouche and V. Girault. Problèmes généralisés de Stokes. *Portugal. Math.*, 49(4):463–503, 1992.

[7] C. Amrouche and V. Girault. Decomposition of vector spaces and application to the Stokes problem in arbitrary dimension. *Czechoslovak Math. J.*, 44(119)(1):109–140, 1994.

[8] M. Badra, F. Caubet, and M. Dambrine. Detecting an obstacle immersed in a fluid by shape optimization methods. *M3AS*, HAL-00583469, 2011.

[9] A. Ballerini. Stable determination of an immersed body in a stationary Stokes fluid. *Inverse Problems*, 26(12):125015, 25, 2010.

[10] A. Ballerini. Stable determination of a body immersed in a fluid: the nonlinear stationary case. *Appl. Anal.*, to appear.

[11] A. Ben Abda, M. Hassine, M. Jaoua, and M. Masmoudi. Topological sensitivity analysis for the location of small cavities in Stokes flow. *SIAM J. Control Optim.*, 48(5):2871–2900, 2009/10.

[12] F. Boyer and P. Fabrie. *Éléments d'analyse pour l'étude de quelques modèles d'écoulements de fluides visqueux incompressibles*, volume 52 of *Mathématiques & Applications (Berlin) [Mathematics & Applications]*. Springer-Verlag, Berlin, 2006.

[13] D. Bucur and G. Buttazzo. *Variational methods in shape optimization problems*. Progress in Nonlinear Differential Equations and their Applications, 65. Birkhäuser Boston Inc., Boston, MA, 2005.

[14] C. Conca, P. Cumsille, J. Ortega, and L. Rosier. Detecting a moving obstacle in an ideal fluid by a boundary measurement. *C. R. Math. Acad. Sci. Paris*, 346(15-16):839–844, 2008.

[15] C. Conca, M. Malik, and A. Munnier. Detection of a moving rigid solid in a perfect fluid. *Inverse Problems*, 26(9):095010, 18, 2010.

[16] M. Dambrine. On variations of the shape Hessian and sufficient conditions for the stability of critical shapes. *RACSAM Rev. R. Acad. Cienc. Exactas Fís. Nat. Ser. A Mat.*, 96(1):95–121, 2002.

[17] M. Engliš and J. Peetre. A Green's function for the annulus. *Ann. Mat. Pura Appl. (4)*, 171:313–377, 1996.

[18] G. P. Galdi. *An introduction to the mathematical theory of the Navier-Stokes equations.*, volume 38 of *Springer Tracts in Natural Philosophy*. Springer-Verlag, New York, 1994. Linearized steady problems.

[19] S. Garreau, P. Guillaume, and M. Masmoudi. The topological asymptotic for PDE systems: the elasticity case. *SIAM J. Control Optim.*, 39(6):1756–1778 (electronic), 2001.

[20] A. Henrot and M. Pierre. *Variation et optimisation de formes*, volume 48 of *Mathématiques & Applications (Berlin) [Mathematics & Applications]*. Springer, Berlin, 2005. Une analyse géométrique. [A geometric analysis].

[21] D. Martin. Finite Element Library MÉLINA. `http://homepage.mac.com/danielmartin/melina/`.

[22] V. Maz′ya and T. Shaposhnikova. *Theory of multipliers in spaces of differentiable functions*, volume 23 of *Monographs and Studies in Mathematics*. Pitman (Advanced Publishing Program), Boston, MA, 1985.

[23] F. Murat and J. Simon. *Sur le contrôle par un domaine géométrique*. Rapport du L.A. 189, 1976. Université de Paris VI, France.

[24] J. Nocedal and S. J. Wright. *Numerical optimization*. Springer Series in Operations Research and Financial Engineering. Springer, New York, second edition, 2006.

[25] J. R. Shewchuk. Mesh Generator TRIANGLE. `http://www.cs.cmu.edu/~quake/triangle.html`.

[26] J. Simon. Differentiation with respect to the domain in boundary value problems. *Numer. Funct. Anal. Optim.*, 2(7-8):649–687 (1981), 1980.

[27] J. Simon. Second variations for domain optimization problems. In *Control and estimation of distributed parameter systems (Vorau, 1988)*, volume 91 of *Internat. Ser. Numer. Math.*, pages 361–378. Birkhäuser, Basel, 1989.

[28] J. Simon. Domain variation for drag in Stokes flow. In *Control theory of distributed parameter systems and applications (Shanghai, 1990)*, volume 159 of *Lecture Notes in Control and Inform. Sci.*, pages 28–42. Springer, Berlin, 1991.

[29] J. Sokołowski and A. Żochowski. On the topological derivative in shape optimization. *SIAM J. Control Optim.*, 37(4):1251–1272 (electronic), 1999.

[30] J. Sokołowski and J.-P. Zolésio. *Introduction to shape optimization*, volume 16 of *Springer Series in Computational Mathematics*. Springer-Verlag, Berlin, 1992. Shape sensitivity analysis.